

New International Formulation for the Viscosity of Heavy Water

Cite as: J. Phys. Chem. Ref. Data **50**, 033102 (2021); <https://doi.org/10.1063/5.0048711>


Submitted: 25 February 2021 • Accepted: 03 June 2021 • Published Online: 08 July 2021

 M. J. Assael,  S. A. Monogenidou,  M. L. Huber, et al.

COLLECTIONS

Paper published as part of the special topic on [International Water Property Standards](#)

 This paper was selected as an Editor's Pick

 This paper was selected as Scilight



View Online



Export Citation



CrossMark

ARTICLES YOU MAY BE INTERESTED IN

[Equations of State for the Thermodynamic Properties of Three Hexane Isomers: 3-Methylpentane, 2,2-Dimethylbutane, and 2,3-Dimethylbutane](#)

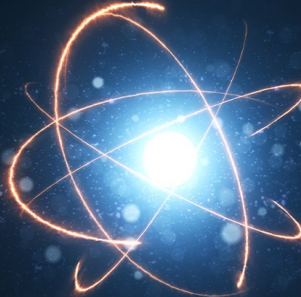
Journal of Physical and Chemical Reference Data **50**, 033103 (2021); <https://doi.org/10.1063/1.5093644>

[CODATA Recommended Values of the Fundamental Physical Constants: 2018](#)

Journal of Physical and Chemical Reference Data **50**, 033105 (2021); <https://doi.org/10.1063/5.0064853>

[A Reference Equation of State for Heavy Water](#)

Journal of Physical and Chemical Reference Data **47**, 043102 (2018); <https://doi.org/10.1063/1.5053993>



Journal of Physical and
Chemical Reference Data

CODATA Recommended Values of the
Fundamental Physical Constants: 2018

READ TODAY!

New International Formulation for the Viscosity of Heavy Water

Cite as: J. Phys. Chem. Ref. Data 50, 033102 (2021); doi: 10.1063/5.0048711

Submitted: 25 February 2021 • Accepted: 3 June 2021 •

Published Online: 8 July 2021



M. J. Assael,¹  S. A. Monogenidou,¹  M. L. Huber,^{2,a)}  R. A. Perkins,²  and J. V. Sengers^{2,3} 

AFFILIATIONS

¹Laboratory of Thermophysical Properties and Environmental Processes, Chemical Engineering Department, Aristotle University, Thessaloniki 54636, Greece

²Applied Chemicals and Materials Division, NIST, Boulder, Colorado 80305, USA

³Institute for Physical Science and Technology, University of Maryland, College Park, Maryland 20742, USA

^{a)}Author to whom correspondence should be addressed: marcia.huber@nist.gov

ABSTRACT

The International Association for the Properties of Water and Steam has recently adopted a new formulation for the thermodynamic properties of heavy water. This manuscript describes the development of a new formulation for the viscosity of heavy water that is consistent with the new equation of state and is valid for fluid states up to 775 K and 960 MPa with uncertainties ranging from 1% to 5% depending on the state point. Comparisons with experimental data and with a previous viscosity formulation are presented. The new formulation contains terms for the enhancement of viscosity in a small region near the critical point that were not included in previous formulations. The new formulation is applicable over a wider range of conditions than previous correlations.

© 2021 by the U.S. Secretary of Commerce on behalf of the United States. All rights reserved. <https://doi.org/10.1063/5.0048711>

Key words: D₂O; dynamic viscosity; heavy water; IAPWS; viscosity.

CONTENTS

1. Introduction	2	Acknowledgments	18
2. Experimental Data	4	6. Data Availability	18
3. Development of the Formulation	5	7. References.	18
3.1. Viscosity in the limit of zero density	5		
3.2. Residual contribution	6		
3.3. Critical region	7		
3.3.1. Theory	7		
3.3.2. Application to D ₂ O	8		
3.3.3. Extrapolation to the critical point	10		
3.3.4. Evaluation of the optimum wavenumber cutoff	10		
3.4. Simplified formulation	11		
3.5. Computer-program verification	11		
3.6. Recommendation for industrial applications	12		
3.7. Liquid D ₂ O at 0.1 MPa	12		
4. Evaluation	14		
4.1. Comparisons with experimental data and the 2007 IAPWS formulation for viscosity	14		
4.2. Range and uncertainty estimates for the formulation	17		
5. Conclusions	18		

List of Tables

1. Summary of experimental data for the viscosity of D ₂ O	3
2. Reference constants	5
3. Coefficients H_{ij} in Eq. (4) for $\bar{\mu}_1(\bar{T}, \bar{p})$	7
4. Sample points for computer-program verification of the correlating equation (2) with $\bar{\mu}_2 = 1$	11
5. Sample points for computer-program verification of the correlating equation (2) in the region near the critical point	12
6. Coefficients a_i and exponents b_i in Eq. (28) for the viscosity of liquid D ₂ O at 0.1 MPa	12
7. Summary of critical region constants	13
8. Summary of comparisons of Eq. (2) with experimental data and the previous 2007 IAPWS formulation for the viscosity	13

List of Figures

1. Temperature–pressure ranges of the primary experimental viscosity data for heavy water	4
2. Temperature–density ranges of the primary experimental viscosity data for heavy water	5
3. Percentage deviations of the experimental viscosity values from those calculated by Eq. (3).	6
4. Dynamic viscosities calculated from the kinematic viscosity data of Rivkin and Romashin ²⁵ with densities calculated from the EOS of Herrig <i>et al.</i> ¹⁴ for D ₂ O.	9
5. Critical enhancement of the viscosity of D ₂ O from the data of Rivkin and Romashin ²⁵ as a function of density.	9
6. Critical enhancement of the viscosity of D ₂ O from the data of Rivkin and Romashin ²⁵ as a function of correlation length.	9
7. The correlation length ξ for D ₂ O as a function of reduced temperature $t = (T - T_c)/T_c$	10
8. The critical enhancement $\bar{\mu}_2$ as a function of reduced temperature t at $\rho = \rho_c$	10
9. Temperature and density regions where the viscosity enhancement $\bar{\mu}_2$ exceeds 1.000 52 (dotted curve) and 1.02 (dashed curve)	11
10. Deviations along selected isotherms between the full model [Eq. (2)] and the simplified model for industrial applications [Eq. (27)]	12
11. Deviations of the primary data at 0.1 MPa from Eq. (28).	12
12. Percentage deviations of the primary experimental data from the present formulation as a function of temperature for pressures below 0.102 MPa	14
13. Percentage deviations of the primary experimental data from the 2007 IAPWS formulation as a function of temperature for pressures below 0.102 MPa	14
14. Percentage deviations of the primary experimental data from the present formulation as a function of temperature for pressures between 0.102 and 100 MPa	14
15. Percentage deviations of the primary experimental data from the 2007 IAPWS formulation as a function of temperature for pressures between 0.102 and 100 MPa	15
16. Percentage deviations of the primary experimental data from the present formulation as a function of temperature for pressures above 100 MPa	15
17. Percentage deviations of the primary experimental data from the 2007 IAPWS formulation as a function of temperature for pressures above 100 MPa	15
18. Percentage deviations of the primary experimental data from the present formulation as a function of density	15
19. Percentage deviations of the primary experimental data from the 2007 IAPWS formulation as a function of density	16
20. Percentage deviations of the primary experimental data from the present formulation as a function of pressure for temperatures below 276.97 K.	16
21. Percentage deviations of the primary experimental data from the 2007 IAPWS formulation as a function of pressure for temperatures below 276.97 K	16
22. Percentage deviations of the primary experimental data from the present formulation as a function of pressure for temperatures between 277 and 500 K	16
23. Percentage deviations of the primary experimental data from the 2007 IAPWS formulation as a function of pressure for temperatures between 277 K and 500 K	17
24. Percentage deviations of the primary experimental data from the present formulation as a function of pressure for temperatures above 500 K	17
25. Percentage deviations of the primary experimental data from the 2007 IAPWS formulation as a function of pressure for temperatures above 500 K	17
26. Expanded uncertainties of the present formulation for the viscosity of heavy water	17

1. Introduction

The properties of heavy water, deuterium oxide (D₂O, CAS No. 7789-20-0), are of interest for a number of applications, including as a neutron moderator and coolant in nuclear reactors¹ and in biological and medical research as a labeling compound. A first survey of some thermophysical and chemical properties of heavy water was published in 1951 in the U.S. in a book by Kirshenbaum.² Following this, in 1963, a comprehensive collection of thermophysical property information, including tables of thermodynamic properties of heavy water, was published by Kazavchinskii and co-workers³ in the Soviet Union.

The activities of the International Association for the Properties of Steam (IAPS), which later became the International Association for the Properties of Water and Steam (IAPWS), started in 1979 on the transport properties of D₂O, when Watson⁴ prepared a formulation for the zero-density viscosity of heavy water valid between 273.15 and 1773.15 K with an estimated uncertainty ranging between 3% and 5%.

In 1980, Nagashima and Matsunaga⁵ proposed the first correlation for the viscosity of heavy water, covering liquid and gaseous states in the temperature range 276.96–773.15 K and up to 100 MPa. Due to an insufficient number of available data on the viscosity in the very narrow region near the critical point (± 1 K and ± 0.1 MPa), they suggested that a critical enhancement be left for future study and they did not propose a term to account for the critical enhancement. Their formulation was proposed to be accurate to $\pm 2\%$ in the entire region except for the vapor region below 373 K, the liquid region near the melting point, and the critical region. For the development of the correlation, the density of D₂O was calculated with the aid of the 1977 equation of state (EOS) of Ikeda *et al.*⁶ in the liquid region up to 100 MPa and with the aid of the modified law of corresponding states and the 1975 EOS for H₂O by Pollak⁷ in all other regions.

In 1982, an EOS for heavy water was developed by Hill *et al.*⁸ Following this, and at the request of the Executive Committee of IAPS, Matsunaga and Nagashima⁹ in 1983 published a new correlation for the viscosity of heavy water. The correlation was formulated as the multiplication of the zero-density viscosity term

TABLE 1. Summary of experimental data for the viscosity of D₂O

First author	Year	Method ^a	Uncertainty ^b (%)	Purity (%)	Number of data	Temp. range (K)	Press. range (MPa)
Primary data							
Issenmann ²²	2019	DDM	2–7	100 ^c	78	244–293	0.1
Harris ²³	2004	FB	1	99.9	128	256–298	0.1–395
Agayev ²⁴	1990	CAP	1.2	99.8	182	263–283	0.1–216
Rivkin ²⁵	1986	CAP	1	99.93	57	645–673	12–28
Kestin ²⁶	1985	OSD	0.2	99.75	72	298–493	sat–30
Agayev ^{27 d}	1980	CAP	0.5–1.5	99.8	172	277–645	0.1–196
Gonçalves ^{28 d}	1980	CAP	0.1	99.75	6	293–333	0.1
Rivkin ^{29 d}	1980	CAP	1	na	71	523–643	2–21.5
Abe ^{30 d}	1978	CAP	1.5	99.8	40	473–673	0.1–20
Kinoshita ^{31,32 d}	1978	CAP	0.5	99.87	50	323–773	5–78
Osipov ³³	1977	CAP	1.5–3	98	26	242–277	0.1
Kellomäki ^{34 d}	1975	CAP	0.1	99.8	6	283–308	0.1
Rivkin ^{35–37 d}	1975	CAP	1	na	50	323–773	10–50
Rivkin ^{38 d}	1974	CAP	1	na	69	473–648	sat–50
Timrot ^{39 d}	1974	OSD	0.35	99.5	15	375–778	0.008–0.13
Agayev ^{40 d}	1971	CAP	1	99.8	157	373–548	0.1–118
Miller ^{41 d}	1971	CAP	na	99.88	28	278–343	0.1
Selecki ^{42 d}	1970	CAP	0.8	99.8	6	298–363	0.1
Agayev ^{43 d}	1968	CAP	0.5	99.8	257	277–423	0.1–118
Harlow ⁴⁴	1967	FB	1.4	99.7	96	283–373	0.1–964
Bonilla ⁴⁵	1956	CAP	0.3	99.8	15	473–1775	0.1
Secondary data							
Frost ⁴⁶	2020	DDM	4	99.9	16	297	100–1470
DeFries ⁴⁷	1977	RB	2	99.77	36	258–283	0.1–600
Kudish ^{48,49}	1975	CAP	0.2	94.83 ^e	10	288–308	0.1
Lee ⁵⁰	1972	RB	2	99.8	55	283–363	1.5–467
Timrot ⁵¹	1959	CAP	0.5	na	24	288–561	4.5–32
Heike ⁵²	1954	FB	3	99.2	12	303–523	0.1–4
Hardy ^{53,54}	1949	CAP	0.25	99.5	11	278–398	0.1–0.3
Lemondé ⁵⁵	1941	CAP	na	99.65	17	277–293	0.1
Jones ⁵⁶	1936	CAP	na	97.6	1	298	0.1
Baker ⁵⁷	1935	CAP	na	98 ^c	1	298	0.1
Taylor ⁵⁸	1934	CAP	na	na	1	293	0.1
Lewis ⁵⁹	1933	CAP	0.5	90 ^c	7	278–308	0.1
Selwood ⁶⁰	1933	CAP	na	92 ^c	1	293	0.1

^aCAP: Capillary, DDM: Dynamic differential microscopy, FB: Falling body, OSD: Oscillating disk, and RB: Rolling body.^bna: Not available.^cValue extrapolated to 100% by the original authors.^dMeasurements employed by Matsunaga and Nagashima.⁹^eFor isotope D₂¹⁸O, not considered further here.

and a residual term while the critical enhancement was not considered. The zero-density term was based on the aforementioned work of Watson.⁴ The formulation was valid up to 100 MPa and from the triple-point temperature up to 775 K. It was also published together with other properties of D₂O in a paper by Kestin *et al.*¹⁰ and incorporated in the IAPS Release of 1984¹¹ and the Revised IAPWS Release of 2007.¹²

It should also be mentioned that in 1999, Aleksandrov and Matveev¹³ proposed a formulation for the viscosity of heavy water, including additional viscosity data that were not available in 1983. Similar to Matsunaga and Nagashima,⁹ they did not include a critical enhancement.

In 2018, a new EOS for heavy water was developed by Herrig *et al.*¹⁴ and incorporated in the Revised IAPWS Release of 2017.¹⁵ The new EOS describes the density near the critical point accurately, which allows for the initial calculation of the viscosity critical enhancement. This new EOS, the availability of new measurements of the viscosity of heavy water performed after 1983, and a much better understanding of the viscosity critical enhancement were part of the motivation for the development of an improved correlation for the viscosity of heavy water in this work. In addition, advances in the calculation of the zero-density viscosity by Hellmann and Bich¹⁶ can now be incorporated. The new formulation provided in this work is

recommended for calculating the viscosity of heavy water, which IAPWS defines as water whose hydrogen atoms are entirely the deuterium isotope (^2H or D) and whose oxygen isotopes have the same abundance as in ordinary water.¹⁷ The new formulation for the viscosity of heavy water described in this work has recently been adopted by IAPWS as an international standard;¹⁸ one of the purposes of this manuscript is to document the new standard.

We follow a procedure adopted by Matsunaga and Nagashima⁹ (also used in our previous formulation of the viscosity of water¹⁹) that is applied to the best available experimental data. The analysis begins with a critical assessment of the experimental data for viscosity. For this purpose, two categories of experimental data have been defined: primary data employed in the development of the correlation, and secondary data used simply for comparison purposes. According to the recommendation adopted by the Subcommittee on Transport Properties (now known as the International Association for Transport Properties) of the International Union of Pure and Applied Chemistry (IUPAC), the primary data are identified by a well-established set of criteria.²⁰ These criteria have been successfully employed to establish standard reference values for the viscosity and thermal conductivity of fluids over wide ranges of conditions, with uncertainties in the range of 1%. However, in many cases, such a narrow definition unacceptably limits the range of the data representation. Hence, within the primary dataset, it is also necessary to include results that extend over a wide range of conditions, albeit with a higher uncertainty, provided that they are consistent with other lower uncertainty data or with theory. In all cases, the uncertainty claimed for the final recommended data must reflect the estimated uncertainty in the primary information.

2. Experimental Data

In 1983, Matsunaga and Nagashima⁹ reviewed the data available at the time. Later, Assael *et al.*²¹ built upon that work and, as part of a joint project between IAPWS and the International Association for Transport Properties, collected experimental data on the viscosity of heavy water and converted the data to the ITS-90 temperature scale and a common set of units. A few datasets were recalculated, and the modifications will be discussed later. Unless the temperature scale was explicitly stated in a publication or additional information was available, the year of publication was used to determine the appropriate temperature scale for the conversion.

In this work, we have employed all the data examined by Matsunaga and Nagashima⁹ in 1983 and considered six sets of measurements performed after that date. Table 1 summarizes all available datasets; 34 papers were considered totaling 1773 viscosity measurements. The temperature range covered is from 242 to 778 K (with one dataset at 0.1 MPa extending to 1775 K) and up to 1470 MPa. In the same table, the technique employed, the uncertainty as quoted by the original authors, and the purity of the sample are also shown. It should be noted that the uncertainties as given by the original authors are often unclear on the coverage factor used and may not all be on the same basis.

From the 34 datasets presented in Table 1, 21 sets were considered as primary data to be used for the development of the formulation. These include the 13 datasets employed in the previous viscosity formulation of Matsunaga and Nagashima⁹ (marked in the table by a superscript d) and 8 more. Also included are the

measurements of Osipov *et al.*³³ that were performed in a capillary viscometer down to 242 K, with an uncertainty of 1.5%–3%. As there are few supercooled measurements, these were considered as primary data. The recalculated viscosities from the measurements of Bonilla *et al.*⁴⁵ (to be discussed in Sec. 3.1) were also included as they are the only ones extending to very high temperatures. These were performed in a capillary viscometer with 0.3% quoted uncertainty. The measurements of Harlow⁴⁴ were made with a falling-cylinder apparatus and were included in the primary dataset in order to extend the pressure range, as these measurements extend to 960 MPa. The experimental measurements in the remaining five datasets were performed after the aforementioned formulation. The measurements of Kestin *et al.*²⁶ were performed in an oscillating-disk viscometer with an uncertainty of 0.2%. Agayev²⁴ and Harris and Woolf²³ performed measurements that extended to high pressures at low temperatures with 1% uncertainty with a capillary viscometer and a falling-body viscometer, respectively. Very recently, Issenmann and Caupin²² performed measurements employing a dynamic differential technique on metastable supercooled heavy water. Finally, Rivkin and Romashin²⁵ published high-temperature measurements obtained using a capillary viscometer with 1% uncertainty. All these datasets were included in the primary data. In addition, the very recent data of Frost and Glenzer⁴⁶ came to our attention after the development of the formulation and thus were not included in the development but are included as secondary data and are used for comparisons. The measurements, all at 24 °C, extend to extremely high pressures (up to 1470 MPa) and were performed with an experimental technique incorporating differential dynamic microscopy.

Figures 1 and 2 show the temperature–pressure ranges and the temperature–density ranges of the primary experimental data listed in Table 1. We will formulate the correlation as a function of temperature and density, in part, because there is a theoretical basis for such a form for the transport properties of moderately dense gases and for the critical region. Typically, experimental viscosity measurements are presented at specified temperatures and pressures, and it is

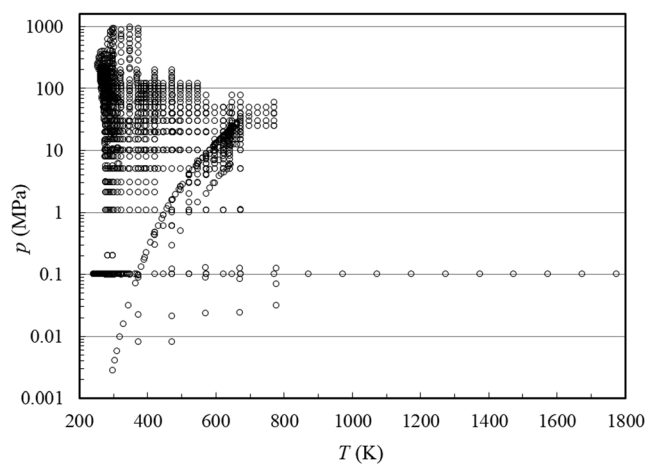


FIG. 1. Temperature–pressure ranges of the primary experimental viscosity data for heavy water.

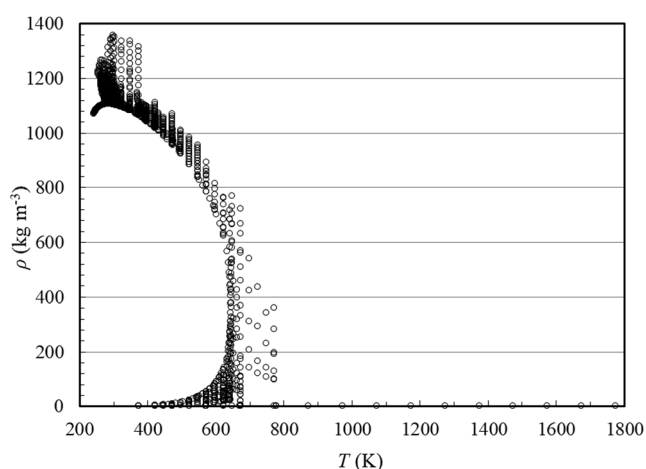


FIG. 2. Temperature–density ranges of the primary experimental viscosity data for heavy water.

therefore necessary to use an EOS to obtain the value of density corresponding to an experimental T, p state point. We use the recently developed accurate, wide-ranging EOS developed by Herrig *et al.*¹⁴ that is valid from the triple point up to 825 K and 1000 MPa. In the homogenous liquid and vapor phases, the expanded relative uncertainties of densities calculated from the EOS are mostly within 0.1%; liquid-phase densities at atmospheric pressure can be calculated with an uncertainty of 0.01%. We also adopt the values for the critical point from Herrig *et al.*¹⁴ The critical temperature, T_c , the critical pressure, p_c , and the critical density, ρ_c , are 643.847 K, 21.6618 MPa, and 356.00 kg m⁻³, respectively.¹⁴ The triple-point temperature employed is 276.969 K, and the molar mass is 20.027 508 g mol⁻¹.¹⁴ The primary dataset contains some data in the metastable supercooled region, which is not explicitly covered by the EOS of Herrig *et al.*¹⁴ For points below the triple point at atmospheric pressure in the metastable supercooled region, we use the work of Duška *et al.*⁶¹ to provide density; this was applied to the data of Issenmann and Caupin²² and of Osipov *et al.*³³ that require densities at temperatures as low as 242 K at atmospheric pressure. We note that recently, we became aware of another publication that also deals with the density of supercooled heavy water.⁶²

3. Development of the Formulation

In order to provide consistency with the conventions adopted by IAPWS in their releases on the transport properties of water and heavy water, we use the following dimensionless variables for temperature T , mass density ρ , pressure p , and viscosity μ :

TABLE 2. Reference constants

Constant	Value
T^*	643.847 K
ρ^*	356.0 kg m ⁻³
p^*	21.6618 MPa
μ^*	1×10^{-6} Pa s

$$\bar{T} = \frac{T}{T^*}, \quad \bar{\rho} = \frac{\rho}{\rho^*}, \quad \bar{p} = \frac{p}{p^*}, \quad \bar{\mu} = \frac{\mu}{\mu^*}, \quad (1)$$

where the reference constants are given in Table 2. The reference values for temperature, pressure, and density are the critical parameters of the IAPWS reference EOS for heavy water,¹⁴ while $\mu^* = 1 \times 10^{-6}$ Pa s is the scale factor previously adopted by IAPWS for the viscosity of H₂O.¹⁹ All temperatures are expressed in terms of the ITS-90 temperature scale.

The formulation for the viscosity of heavy water has the same general form as the current formulation for the viscosity of water,¹⁹ namely,

$$\bar{\mu} = \bar{\mu}_0(\bar{T}) \times \bar{\mu}_1(\bar{T}, \bar{\rho}) \times \bar{\mu}_2(\bar{T}, \bar{\rho}). \quad (2)$$

The first factor $\bar{\mu}_0$ of the product represents the viscosity in the zero-density limit and is a function of temperature only. The second factor $\bar{\mu}_1$ represents the residual contribution to viscosity (due to increasing density), while the third factor $\bar{\mu}_2$ represents an enhancement of the viscosity near the critical point. The determination of each of these contributions will be considered in Secs. 3.1–3.3.

3.1. Viscosity in the limit of zero density

In 2017, Hellmann and Bich¹⁶ applied the classical kinetic theory of polyatomic gases to calculate the traditional transport properties of heavy water in the zero-density limit using two highly accurate *ab initio* pair potentials. Results were reported for shear viscosity, thermal conductivity, and the product of molar density and self-diffusion coefficient at temperatures between 250 and 2500 K. The expanded uncertainty (coverage factor $k = 2$) of the computed values for the viscosity is estimated to be 2%. Due to the lack of a large amount of high-quality experimental data for heavy water, we chose to base the zero-density correlation on the calculations of Hellmann and Bich¹⁶ alone and only compare with the experimental data; this is different than the approach taken for ordinary water.^{19,63} In order to cover the entire temperature range from 250 to 2500 K, we fitted the viscosity values to the following empirical form, as a function of the dimensionless temperature \bar{T} :

$$\bar{\mu}_0(\bar{T}) = \sqrt{\bar{T}} \frac{0.889\,754 + 61.222\,17\,\bar{T} - 44.8866\,\bar{T}^2 + 111.5812\,\bar{T}^3 + 3.547\,412\,\bar{T}^4}{0.796\,37 + 2.381\,27\,\bar{T} - 0.334\,63\,\bar{T}^2 + 2.669\,\bar{T}^3 + 0.000\,211\,366\bar{T}^4}. \quad (3)$$

Equation (3) agrees to within 0.05% with all values given by Hellmann and Bich¹⁶ over the temperature range 250–2500 K. As mentioned above, the values given by Hellmann and Bich¹⁶ have an estimated uncertainty of 2%.

Equation (3) was tested vs the available experimental data. The following sets were employed:

- Rivkin *et al.*²⁹ and Agayev²⁷ performed capillary measurements in the vapor phase, with an uncertainty of 1% and 1.5%, respectively. As both these investigators measured the viscosity along specific isotherms, it was easy to extrapolate their measurements to zero density with a linear function.
- Abe *et al.*³⁰ also performed capillary measurements in the vapor phase with an uncertainty of 1.5%, but at 0.1 MPa. These values were incorporated as zero-density values, introducing a maximum additional uncertainty of 0.2%.
- Timrot *et al.*³⁹ employed an oscillating-disk viscometer for measurements in the vapor phase, with an uncertainty of 0.35%. They measured at very low pressures, well below 0.03 MPa, and thus, their measurements at the lowest pressure were considered as zero-density values. This introduced an additional error of ~0.1%.
- Finally, Bonilla *et al.*⁴⁵ employed a capillary viscometer for measurements in the vapor phase from 473 to 1775 K, at 0.1 MPa, with a quoted uncertainty of 0.3%. Values at 0.1 MPa were employed, introducing a 0.2% uncertainty. Furthermore, they calibrated their instrument with nitrogen employing the 1945 values measured by Vasilescu.⁶⁴ Since the calibration procedure was given in their publication, we recalculated their viscosity values employing more up-to-date nitrogen values.⁶⁵

In Fig. 3, the deviations of the experimental viscosity values from those calculated by Eq. (3) are shown. The agreement is within 2% except for data at the lowest four temperatures examined by Bonilla *et al.*⁴⁵ that also deviate slightly from the other data in this region. In the same figure, the deviations of the 2007 IAPWS viscosity formulation¹² from

the values calculated by Eq. (3) are also shown. The agreement is excellent down to 280 K, where the deviations begin to exceed 3%.

Therefore, Eq. (3) is considered sufficient to represent the zero-density viscosity of heavy water from 250 to 2500 K with an uncertainty of 2% (at the 95% confidence level). However, we note that at very high temperatures (above about 2100 K for steam⁶⁶), dissociation may occur. The present equation does not account for dissociation; one may wish to consider these effects, as discussed in Refs. 66 and 67.

3.2. Residual contribution

The second factor $\bar{\mu}_1$ of the product in Eq. (2) is the residual viscosity and represents the contribution to viscosity due to increasing density. This term is frequently referred to in the literature as excess viscosity,⁶⁸ but here we follow the alternative nomenclature of residual viscosity.⁶⁹ The critical region is not considered here; it will be treated separately in Sec. 3.3. We adopt the same general form for $\bar{\mu}_1$ as in the previous IAPWS formulation for D₂O^{9,10,12} and also for ordinary water,¹⁹

$$\bar{\mu}_1(\bar{T}, \bar{\rho}) = \exp \left[\bar{\rho} \sum_{i=0}^6 \left(\frac{1}{\bar{T}} - 1 \right)^i \sum_{j=0}^6 H_{ij} (\bar{\rho} - 1)^j \right], \quad (4)$$

with coefficients H_{ij} to be determined by regression of experimental data.

All data were initially assigned weights $1/u^2$, where u is the estimated experimental uncertainty. The uncertainties are given in Table 1 and are as given in the original author's recommendation unless noted otherwise. As discussed earlier in Sec. 2, all densities were computed with the EOS of Herrig *et al.*¹⁴ except for the metastable supercooled region where the densities were obtained from Ref. 61.

Equation (4) contains a maximum of 49 empirical terms; there is no theoretical motivation for the form or the total number of terms necessary or which terms will best represent the experimental data. Following a procedure in our previous work,¹⁹ in order to determine the statistically significant terms, we used a simulated annealing procedure⁷⁰ along with the orthogonal distance regression package ODRPACK⁷¹ to arrive at our final formulation. Simulated annealing⁷⁰ is an optimization technique that can be used in complex problems where there may be multiple local minima. It is a combinatorial method that does not require derivatives and does not depend upon “traveling downhill”; it is also relatively easy to implement. In this work, the search space contained a bank of terms corresponding to the terms in Eq. (4) for all values of i and j . The total number of terms was fixed in each optimization experiment, and the simulated annealing algorithm was used to determine the optimal terms from the bank of terms. As in earlier work,⁷² we implemented an annealing schedule recommended by Lundy and Mees.⁷³ Successive runs were made with different total numbers of terms, from 20 to 26. During successive runs, we found it necessary to increase or decrease the weight in some (T, ρ) regions in order to obtain a good representation of the data. In particular, we found it necessary to add additional weight to the data of Harris and Woolf²³ at low temperatures and high pressures and the metastable supercooled region represented by the datasets of Issenmann and Caupin²² and of Osipov *et al.*³³

Although, as mentioned in the previous paragraph, the terms in $\bar{\mu}_1$ are empirical, there is some theoretical guidance on the linear-in-density term⁷⁴ contained in Eq. (4). To ensure that the first density correction in the gas phase, $\mu^{(1)}$, described by Eqs. (5)–(7), behaved in a

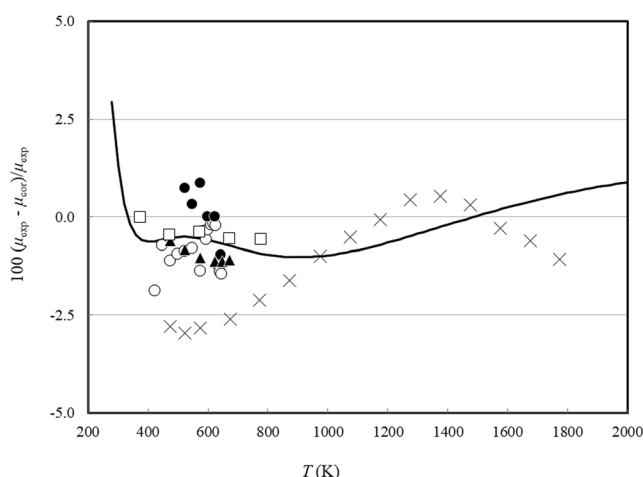


FIG. 3. Percentage deviations of the experimental viscosity values from those calculated by Eq. (3): Agayev²⁷ (○), Rivkin *et al.*²⁹ (●), Abe *et al.*³⁰ (▲), Timrot *et al.*³⁹ (□), and Bonilla *et al.*⁴⁵ (×). The solid curve is the IAPWS 2007 viscosity formulation.¹²

TABLE 3. Coefficients H_{ij} in Eq. (4) for $\bar{\mu}_1(\bar{T}, \bar{\rho})$

i	j	H_{ij}^a
0	0	0.510 953
2	0	−0.558 947
3	0	−2.718 820
4	0	0.480 990
5	0	2.404 510
6	0	−1.824 320
0	1	0.275 847
1	1	0.762 957
3	1	1.760 340
4	1	0.081 908 6
6	1	1.417 750
0	2	−0.228 148
1	2	−0.321 497
5	2	−2.302 500
0	3	0.066 103 5
1	3	0.044 939 3
2	3	1.466 670
5	3	0.938 984
6	3	−0.108 354
0	4	−0.004 812 65
2	4	−1.545 710
3	4	−0.057 093 8
5	4	−0.075 378 3
2	5	0.553 080
2	6	−0.065 020 1

^aCoefficients H_{ij} omitted from Table 3 are identically equal to zero.

reasonable manner, we forced it to approach zero for very large T and to be negative at low temperatures. This is consistent with theoretical approaches.⁷⁴ In addition, since there were few experimental data for $\mu^{(1)}$ for D_2O , we included data for the first density correction for ordinary water¹⁹ into our regressions to guide proper behavior. We make the assumption that the initial density dependence behavior of water is similar to that of heavy water and can be used to assist in obtaining qualitatively correct behavior. One can represent the initial density dependence of the viscosity in the gas phase as

$$\mu^{(1)} = \lim_{\rho \rightarrow 0} \frac{\partial \mu}{\partial \rho} \bigg|_T \quad (5)$$

and for the low-density gas as

$$\mu = \mu_0 + \mu^{(1)} \bar{\rho}. \quad (6)$$

From Eqs. (4) and (5) we obtain

$$\mu^{(1)} = \frac{\mu_0(T)}{\bar{\rho}} \sum_{i=0}^6 H_{i0} \left(\frac{1}{\bar{T}} - 1 \right)^i. \quad (7)$$

We fitted the experimental primary viscosity data for D_2O , listed in Table 1, and the first density correction data for water¹⁹ simultaneously. The objective function was the weighted sum of the squared relative difference between the experimental and calculated values. The relative weight of the first density correction was adjusted until $\mu^{(1)}$ had the desired behavior but did not significantly degrade the fit of the viscosity data. Although Matsunaga and Nagashima⁹

used 26 terms, we found that a 25-term solution adequately represented the data. As mentioned above, we investigated using 20–26 terms and selected 25 since a further reduction in the total number of terms degraded the fit, while increasing the number above 25 did not provide significant improvement. The final values of the coefficients for the residual function are given in Table 3. A detailed comparison of the formulation with experimental data will be presented in Sec. 4.

3.3. Critical region

3.3.1. Theory

The treatment of the viscosity of D_2O in the critical region closely follows the work by IAPWS for the viscosity of H_2O in the critical region.¹⁹ In the vicinity of a critical point, fluids exhibit large fluctuations in the order parameter associated with the critical phase transition. For pure fluids near the vapor–liquid critical point, the order parameter can be asymptotically identified with the density and the corresponding ordering field with the chemical potential. Consequently, the behavior of thermodynamic and transport properties becomes singular at the critical point. Asymptotically close to the critical point, this singular behavior can be described by power laws with universal critical exponents.⁷⁵

A susceptibility χ may be defined as the derivative of the order parameter with respect to the ordering field. In terms of dimensionless variables, the susceptibility is related to the isothermal compressibility such that $\bar{\chi} = \bar{\rho}(\partial \bar{\rho} / \partial \bar{p})_T$.⁷⁶ The spatial extent of the fluctuations is characterized by a correlation length ξ .⁷⁷ Along the critical isochore $\bar{\rho} = 1$ at $\bar{T} \geq 1$, the correlation length ξ and the susceptibility $\bar{\chi}$ diverge as a function of $t = (\bar{T} - 1)/T$ according to power laws of the form

$$\xi \approx \xi_0 t^{-\nu} \text{ and } \bar{\chi} \approx \Gamma_0 t^{-\gamma}, \quad (8)$$

where ξ_0 and Γ_0 are system-dependent amplitudes and ν and γ are universal critical exponents. In this paper, we use the symbol \approx to designate equality asymptotically close to the critical point. For the universal critical exponents, we have continued to adopt the values in Eq. (9) that were previously used in a comprehensive analysis of the thermodynamic properties of H_2O and D_2O ⁷⁸ and adopted in the IAPWS correlations for the transport properties of H_2O .¹⁹ These values are consistent with a subsequent review of the subject,⁷⁹

$$\nu = 0.630 \text{ and } \gamma = 1.239. \quad (9)$$

From Eq. (8), it follows that

$$\xi \approx \xi_0 (\bar{\chi} / \Gamma_0)^{\nu/\gamma}. \quad (10)$$

Although Eq. (10) is strictly valid only for $\rho = \rho_c$, it is also used as an approximation for $\rho \neq \rho_c$.⁸⁰ The viscosity is predicted to diverge as^{81,82}

$$\bar{\mu} \approx \bar{\mu}_b (Q_0 \xi)^{x_\mu}, \quad (11)$$

where Q_0 is an effective wavenumber that determines the amplitude of the power-law divergence of the viscosity, while x_μ is a universal dynamic critical exponent, for which we have adopted the most recent theoretical value⁸³

$$x_\mu = 0.068. \quad (12)$$

In Eq. (11), $\bar{\mu}_b$ is the so-called background viscosity, *i.e.*, the viscosity in the absence of any critical fluctuations. From Eq. (2), it follows that

$$\bar{\mu}_b(\bar{T}, \bar{\rho}) = \bar{\mu}_0(\bar{T}) \times \bar{\mu}_1(\bar{T}, \bar{\rho}). \quad (13)$$

The viscosity exhibits a multiplicative critical anomaly, i.e., the critical enhancement is proportional to the background viscosity $\bar{\mu}_b$.^{82,84}

Equation (11) represents the divergent behavior of the viscosity asymptotically close to the critical point. To apply the theory to experimental data, one needs a theoretically based “crossover” equation that incorporates not only the asymptotic power law given by Eq. (11) but also reduces to the normal background viscosity $\bar{\mu}_b$ away from the critical point. This problem has been solved by Bhattacharjee and co-workers,^{81,85} who derived the following crossover equation to include the critical behavior of the viscosity:

$$\bar{\mu} = \bar{\mu}_b \times \bar{\mu}_2 \text{ with } \bar{\mu}_2 = \exp(x_\mu Y). \quad (14)$$

The function Y is defined by

$$Y = \frac{1}{12} \sin(3\psi_D) - \frac{1}{4q_C\xi} \sin(2\psi_D) + \frac{1}{(q_C\xi)^2} \left[1 - \frac{5}{4}(q_C\xi)^2 \right] \sin(\psi_D) - \frac{1}{(q_C\xi)^3} \left\{ \left[1 - \frac{3}{2}(q_C\xi)^2 \right] \psi_D - \left| (q_C\xi)^2 - 1 \right|^{3/2} L(w) \right\}, \quad (15)$$

with

$$\psi_D = \arccos \left[\left(1 + q_D^2 \xi^2 \right)^{-1/2} \right] \quad (16)$$

and with the function $L(w)$ given by

$$L(w) = \begin{cases} \ln \frac{1+w}{1-w} & \text{for } q_C\xi > 1 \\ 2 \arctan |w| & \text{for } q_C\xi \leq 1 \end{cases}. \quad (17)$$

The variable w is defined as

$$w = \left| \frac{q_C\xi - 1}{q_C\xi + 1} \right|^{1/2} \tan\left(\frac{\psi_D}{2}\right). \quad (18)$$

The function Y contains two system-dependent constants, namely, the wavenumbers q_C and q_D . Asymptotically close to the critical point, i.e., in the limit of large ξ , Eq. (14) reproduces Eq. (11) with an amplitude Q_0 that is related to q_C and q_D such that⁸⁵

$$Q_0^{-1} = (q_C^{-1} + q_D^{-1})e^{4/3}/2. \quad (19)$$

The wavenumber q_C is related to a background contribution to the decay rate of the critical fluctuations and is given by

$$q_C = \frac{k_B T_c^2}{16\mu_b^c \lambda_b^c p_c} \frac{\Gamma_0}{\xi_0^2} \left(\frac{\partial p}{\partial T} \right)_{\rho=\rho_c}^2, \quad (20)$$

where k_B is Boltzmann's constant and μ_b^c and λ_b^c are the values of the background viscosity and background thermal conductivity, respectively, at the critical point, while $(\partial p/\partial T)_{\rho=\rho_c}$ is the slope of the critical isochore at the critical temperature. The wavenumber q_D represents a “Debye” cutoff of the mode-coupling integrals for critical dynamics and is the only adjustable parameter in the theory.

For small ξ , the function Y approaches zero so that $\bar{\mu}$ approaches $\bar{\mu}_b$ in this limit. Around $\xi = 0$, the function Y has a Taylor expansion of the form

$$Y = \frac{1}{5} q_C \xi (q_D \xi)^5 \left(1 - q_C \xi + (q_C \xi)^2 - \frac{765}{504} (q_D \xi)^2 \right). \quad (21)$$

The approximations in the derivation of Eq. (14) for the critical enhancement of the viscosity have been discussed by Luettmmer-Strathmann *et al.*⁸⁶ One of the approximations is that the isobaric specific heat capacity c_p in the mode-coupling integral for the viscosity has been replaced by the difference $c_p - c_v$, where c_v is the isochoric specific heat capacity. These approximations are well-justified in the small region around the critical point where a critical viscosity enhancement is observed.

Equation (10) represents the behavior of the correlation length ξ near the critical point. In the theory of critical phenomena, ξ is to be interpreted as that part of the actual correlation length associated with the long-range critical fluctuations. Hence, the correlation length ξ in Eq. (15) should vanish far away from the critical point. To accomplish this goal, we have adopted a procedure proposed by Olchowy and Sengers⁸⁷ by generalizing Eq. (10) to

$$\xi = \xi_0 \left(\frac{\Delta\bar{\chi}}{\Gamma_0} \right)^{1/\gamma} \quad (22)$$

in terms of $\Delta\bar{\chi}$ (≥ 0), which is defined by

$$\Delta\bar{\chi} = \left[\bar{\chi}(\bar{T}, \bar{\rho}) - \bar{\chi}(\bar{T}_R, \bar{\rho}) \frac{\bar{T}_R}{\bar{T}} \right]. \quad (23)$$

In Eq. (23), \bar{T}_R is a reference temperature sufficiently high above the critical temperature where the critical fluctuations can be assumed to be small. In practice, one may select $\bar{T}_R = 1.5$.^{86–88} Furthermore, $\Delta\bar{\chi}$ is to be taken to be zero when the right-hand side of Eq. (23) becomes negative. This procedure assures that the correlation length ξ in Eqs. (15) and (21) will vanish far away from the critical point, while Eq. (22) still reduces to Eq. (10) asymptotically close to the critical point.

An accurate experimental determination of the viscosity of fluids near their critical point is hampered by the presence of gravitationally induced density gradients.⁸⁹ To avoid this complication, the viscosity of xenon near the critical density and critical temperature has been measured by Berg *et al.*⁹⁰ at low-gravity conditions in the Space Shuttle. In the hydrodynamic limit of zero frequency, the experimental viscosity data are well represented by Eq. (14) with an experimental value for the critical exponent x_μ that agrees with the theoretical value 0.068 within its uncertainty. We conclude that the crossover [Eq. (14)] for the critical behavior of the viscosity has a sound theoretical basis and has been validated experimentally.

3.3.2. Application to D₂O

The critical temperature, density, and pressure for D₂O are those consistent with the IAPWS reference EOS for heavy water¹⁴ and are identical to the reference constants given in Table 2. The amplitudes in Eq. (8) for the correlation length ξ and the dimensionless susceptibility $\bar{\chi}$ of D₂O are

$$\xi_0 = 0.13 \text{ nm}, \quad \Gamma_0 = 0.06. \quad (24)$$

These amplitudes for the correlation length and the dimensionless susceptibility are the same for D₂O and H₂O, as originally shown by Kostrowicka Wyczalkowska *et al.*⁷⁸ We have used these same values for our analysis of H₂O.^{19,91} The wavenumber q_C is given by Eq. (20)

with the relevant properties for D₂O. From the previous correlation for the transport properties of D₂O,¹² it is found that $\lambda_b^c = 204 \text{ mW m}^{-1} \text{ K}^{-1}$, while the present correlation for the background viscosity of D₂O gives $\mu_b^c = 40.023 \text{ } \mu\text{Pa s}$. From the EOS of Herrig *et al.*,¹⁴ it is found that $(\partial p/\partial T)_{\rho=\rho_c} = 0.270 \text{ MPa K}^{-1}$. The properties for D₂O are substituted into Eq. (20) to calculate $q_C^{-1} = 1.9 \text{ nm}$, which is the same cutoff value found for H₂O.^{19,91} All information required for calculation of the critical viscosity enhancement is now available, except for the system-dependent wavenumber q_D , which is optimized to best fit reliable viscosity data in the critical region.

A detailed experimental study of the viscosity of D₂O in the critical region was completed by Rivkin and Romashin.²⁵ In these experiments, the kinematic viscosity μ/ρ was determined by measuring the flow rate through a platinum capillary, which had an internal diameter of 0.3 mm and a length of 50 cm, as a function of the pressure drop over the capillary.^{25,92} The temperature uncertainty ($k = 2$) was estimated at $\pm 0.03 \text{ K}$, while the pressure uncertainty was estimated at $\pm 0.01 \text{ MPa}$.²⁵ In principle, the method can lead to some complications due to the large compressibility near the critical point.^{93–96} However, as they did for H₂O, the investigators made measurements with various pressure differences ranging from 3.3 kPa (25 mm Hg) to 1.2 kPa (9 mm Hg) and verified that the measured kinematic viscosity became independent of the applied pressure difference below 1.6 kPa (12 mm Hg).^{19,91,97} For the measurements on D₂O at densities from 250 to 450 kg m^{-3} , the experiments were conducted with pressure drops of 1.2–1.5 kPa (9–11 mm Hg) that corresponded to Reynolds numbers of 300–500.²⁵ We have adopted the values determined by Rivkin and Romashin for the kinematic viscosity with an uncertainty estimate of $\pm 1\%$ as suggested by the authors.²⁵

Rivkin and Romashin²⁵ obtained the kinematic viscosity as a function of temperature in terms of measured pressures and temperatures on the IPTS-68 scale. We have converted the experimental temperatures to ITS-90, calculated the densities from the EOS of Herrig *et al.*¹⁴ for D₂O, and converted the experimental values for the kinematic

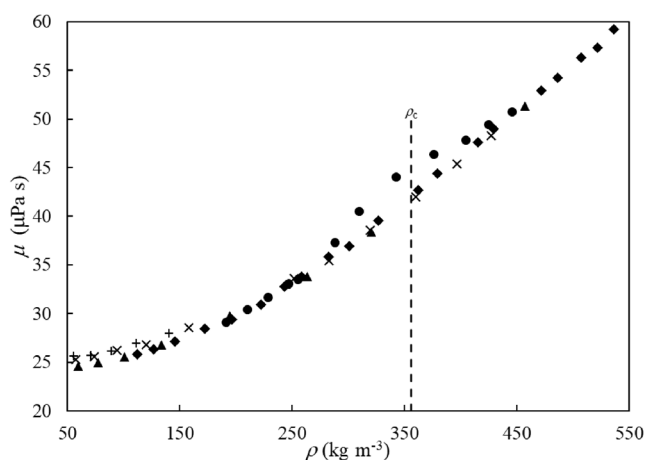


FIG. 4. Dynamic viscosities calculated from the kinematic viscosity data of Rivkin and Romashin²⁵ with densities calculated from the EOS of Herrig *et al.*¹⁴ for D₂O: 645.107 K (●), 647.106 K (◆), 653.106 K (▲), 663.104 K (×), and 673.102 K (+).

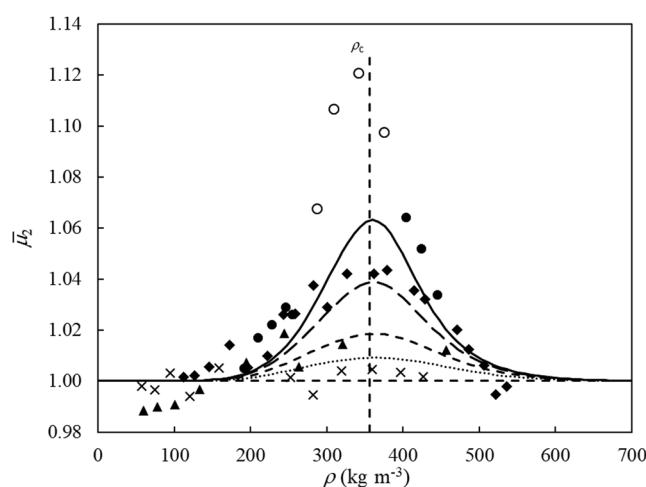


FIG. 5. Critical enhancement of the viscosity of D₂O from the data of Rivkin and Romashin²⁵ as a function of density: 645.107 K (●), 647.106 K (◆), 653.106 K (▲), 663.104 K (×). Equation (14): 645.107 K (solid line), 647.106 K (large dashed line), 653.106 K (small dashed line), and 663.104 K (dotted line).

viscosity μ/ρ into values for the dynamic viscosity μ . Figure 4 shows this dynamic viscosity data as a function of density. A viscosity enhancement is visible in Fig. 4 that is centered about the critical density of 356 kg m^{-3} .

From Eq. (14), it is possible to obtain experimental values for the critical enhancement $\bar{\mu}_2$ from the measured viscosity $\bar{\mu}$ with knowledge of the background viscosity $\bar{\mu}_b$ with its component terms as described in Sec. 3.1 for the dilute gas and in Sec. 3.2 for the residual contributions [see Eq. (13)]. Only the isotherms at 645.107, 647.106, and 653.106 K of Rivkin and Romashin²⁵ are expected to have critical enhancement that exceeds the 1% uncertainty in these data based on the theory for the critical enhancement of viscosity. The Rivkin and

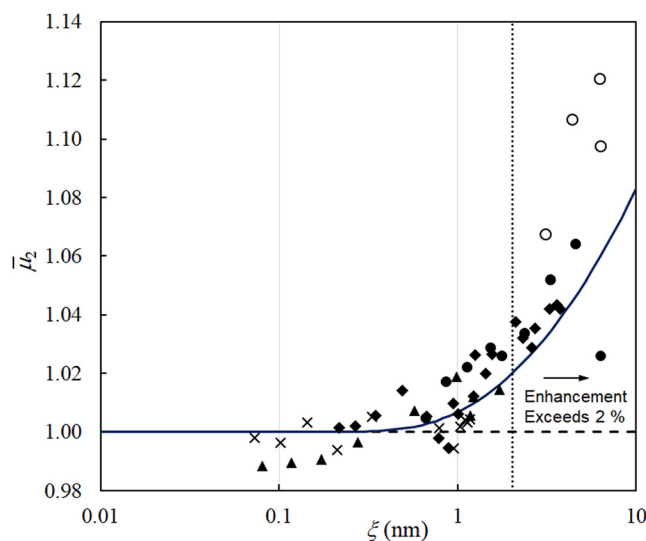


FIG. 6. Critical enhancement of the viscosity of D₂O from the data of Rivkin and Romashin²⁵ as a function of correlation length: 645.107 K (●), 647.106 K (◆), 653.106 K (▲), and 663.104 K (×).

Romashin²⁵ data along the isotherms at 663.104 and 673.102 K were included in the fit for the background viscosity without any contribution for critical enhancement. The resulting background fit was then used to obtain experimental values for the critical enhancement from the data of Rivkin and Romashin.²⁵ The optimum value for q_D^{-1} was found to be 0.4 nm based on the three isotherms with significant critical enhancement at 645.107, 647.106, and 653.106 K. The critical enhancement is shown in Fig. 5 as a function of density. Figure 5 also shows curves calculated from the model with an optimum value for $q_D^{-1} = 0.4$ nm. The experimental critical enhancement is well centered about the critical density so that the experimental temperature is consistent with the critical temperature adopted here. Any temperature shift would also shift the apparent critical enhancement to densities away from the critical density, contrary to theory. The model generally represents the data well, except four data points, denoted by open circles, along the isotherm at 645.107 K near the critical density. These suspect data points indicate a critical enhancement of nearly 13%, while the theoretical model indicates it should be less than 7%, as will be further discussed below.

In applying the theoretical model for the critical viscosity enhancement, we have calculated the correlation length ξ from Eq. (22) using the IAPWS EOS for D₂O.¹⁴ Figure 6 shows the experimental critical enhancement as a function of this correlation length. Again, the four suspect data points exhibit a significantly larger critical enhancement than expected from the theoretical considerations and are depicted as open circles. The solid curve is Eq. (14) with $q_D^{-1} = 0.4$ nm.

3.3.3. Extrapolation to the critical point

The asymptotic power laws are described in Eq. (8) for the correlation length and in Eq. (11) for the critical enhancement of viscosity. The extrapolation behavior of the model described in Secs. 3.3.1 and 3.3.2 will be examined based upon these asymptotic power laws. The classical IAPWS EOS for D₂O¹⁴ has been optimized to describe the thermodynamic properties of D₂O based upon available data, which are sparse very

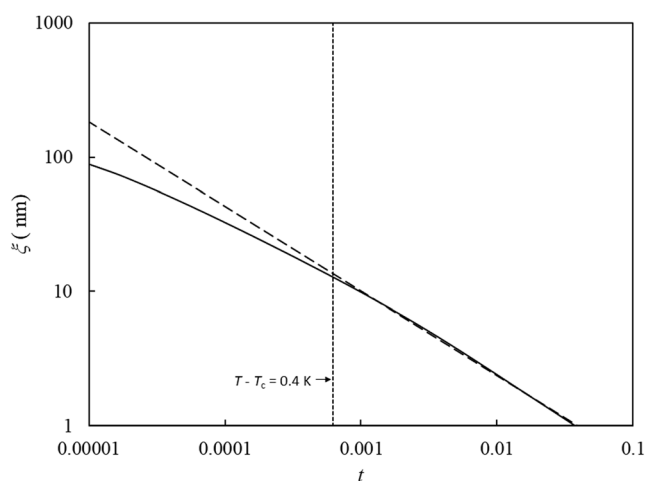


FIG. 7. The correlation length ξ for D₂O as a function of reduced temperature $t = (T - T_c)/T_c$.

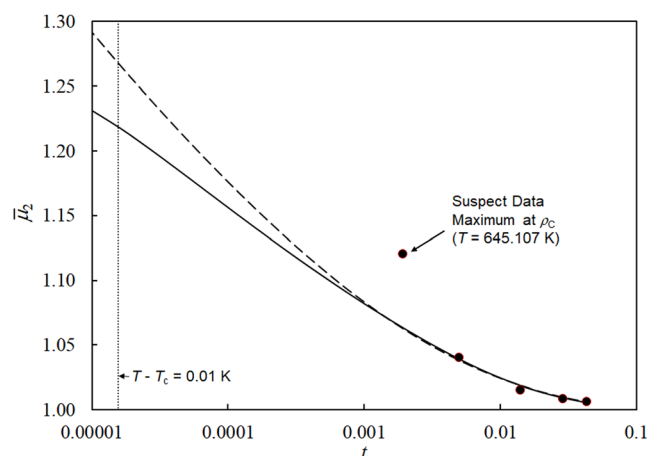


FIG. 8. The critical enhancement $\bar{\mu}_2$ as a function of reduced temperature t at $\rho = \rho_c$.

close to the critical point. Figure 7 shows the correlation length based on this EOS along with that from the asymptotic power law at the critical isochore as a function of $t = (T - T_c)/T_c$. The solid curve is from the EOS of Herrig *et al.*,¹⁴ and the dashed curve is with the asymptotic critical power law $\xi = \xi_0^{t-v}$. The short-dashed vertical line denotes $T - T_c = 0.4$ K. Deviations appear when $T - T_c$ becomes smaller than 0.4 K. Hence, use of the EOS of Herrig *et al.*¹⁴ will restrict our ability to reproduce the divergent behavior of the viscosity within 0.4 K from the critical temperature accurately. Fortunately, the viscosity only diverges as $\xi^{0.068}$ so that the effect of this deficiency remains small at most temperatures of practical interest.

The four experimental values for the viscosity of D₂O from Ref. 25 that appear to be inconsistent can be evaluated relative to the theoretical limiting asymptotic power law for enhancement of viscosity along the critical isochore. The critical enhancement data shown in Fig. 5 can be interpolated for each isotherm at the critical density. These critical enhancement values at the critical density are shown in Fig. 8. In this figure, the solid curve represents crossover theory based on the correlation length ξ from the EOS of Herrig *et al.*,¹⁴ and the dashed curve is the theoretically predicted power-law divergence of the viscosity. It is apparent that the isotherm at 645.107 K exhibits an apparent critical enhancement that is inconsistent with the other isotherms. The other isotherms agree well with the theory with $q_D^{-1} = 0.4$ nm. The asymptotic power law is shown as a dashed line that has been located so that it goes through the experimental value for the isotherm at 647.106 K. The asymptotic power-law slope is the steepest value that the crossover expression can approach. Thus, in contrast to the viscosity near the critical point of H₂O,^{19,91} it is not possible to account for the deviations by a shift of T_c such that a theoretically acceptable line goes through the critical enhancement values for both the isotherms at 645.107 and 647.106 K. We conclude that in this figure, the four outlier data points along the 645.107 K isotherm are not reliable.

3.3.4. Evaluation of the optimum wavenumber cutoff

The only adjustable parameter in the crossover model for the critical enhancement of viscosity is the wavenumber cutoff q_D . As

described in Sec. 3.3.2 and shown in Figs. 5 and 6, the optimum value is given by $q_D^{-1} = 0.4$ nm for the enhancement of D₂O viscosity. Detailed examinations of the viscosity^{19,91} and thermal conductivity⁶³ of H₂O are also available for comparison. For ordinary water, for viscosity,¹⁹ the value of q_D^{-1} is 1.1 nm and for thermal conductivity, q_D^{-1} is 0.4 nm.⁶³

The critical enhancement of the viscosity and thermal conductivity of many fluids has been studied based on crossover theory.^{82,98} Based upon the critical enhancement of thermal conductivity, a simple correlation has been developed for the wavenumber cutoff in terms of the cube root of critical molecular volume. This is given by $q_D^{-1}/\text{nm} = -0.0240 + 0.863v_c^{1/3}/\text{nm}$, where v_c is the molecular volume of the fluid at its critical point.^{82,98} For H₂O at the critical point, $v_c^{1/3} = 0.453$ nm and the correlation predicts $q_D^{-1} = 0.367$ nm. For D₂O at the critical point, $v_c^{1/3} = 0.454$ nm and the correlation predicts $q_D^{-1} = 0.368$ nm. This correlation indicates that there should be an insignificant difference between the wavenumber cutoff for H₂O and D₂O. The correlation agrees well with the experimentally determined values for H₂O thermal conductivity, D₂O thermal conductivity, and D₂O viscosity, but not for H₂O viscosity. The critical enhancement for viscosity is localized, exceeding 2% only within 8.5 K of the critical point where measurements are very difficult. The critical enhancement for thermal conductivity is significant over a much wider range of temperatures and densities.

The viscosity enhancement of Eq. (14) contributes an amount greater than the uncertainty of 2% of our correlation only at states where $\xi > 2.03$ nm. This condition is satisfied only at temperatures and densities within the following boundaries:

$$641.428 \text{ K} < T < 652.259 \text{ K}$$

and

$$243.393 \text{ kg m}^{-3} < \rho < 481.819 \text{ kg m}^{-3}. \quad (25)$$

The dashed curve in Fig. 9 shows where $\bar{\mu}_2 = 1.02$, and the box shows the region given by Eq. (25).

One comment should be made concerning the calculation of the viscosity in the critical region from Eq. (14). While the function Y defined by Eq. (15) does become zero in the limit that ξ goes to zero,

some individual terms diverge in that limit. Hence, Eq. (15) is no longer suitable for numerical calculations at small values of ξ : for $0 \leq \xi \leq 0.03021806692$ nm, Eq. (21) should be used, while for $\xi > 0.03021806692$ nm, Eq. (15) applies. In addition, when $\Delta\bar{\chi}$ calculated by Eq. (23) is less than zero, it must be set to zero for calculations to proceed. Furthermore, due to the numerical implementation of the EOS, the calculated singularity in the first derivative in Eq. (23) may not occur exactly at T_c and ρ_c , as it should. Therefore, depending on the software used, calculated values of $\bar{\mu}_2$ may behave unphysically at points extremely close to the critical point (approximately within 0.01 kg m^{-3} of ρ_c on the critical isotherm). The formulation should be used with caution in this very small region.

3.4. Simplified formulation

Because the critical enhancement of the viscosity contributes less than 2% except in a small region around the critical point between the dashed curve and the phase saturation boundary that is described approximately by Eq. (25) (area inside the rectangular box in Fig. 9), complexity and computing time may be reduced by omitting the critical enhancement for applications outside this region. This can be done by setting $\bar{\mu}_2 = 1$. If a calculation is based upon the crossover model of Eq. (14) near the critical point but uses $\bar{\mu}_2 = 1$ far from the critical point, some discontinuity is inevitable. However, this discontinuity remains less than 0.052% for single-phase states outside a region near the critical point bounded by the equation

$$T/(\text{K}) = \sum_{i=0}^3 a_i [\rho/(\text{kg m}^{-3})]^i, \quad (26)$$

where $a_0 = 4.47555 \times 10^2$, $a_1 = 1.73284$, $a_2 = -3.02766 \times 10^{-3}$, and $a_3 = 1.24296 \times 10^{-6}$. Equation (26) is also shown in Fig. 9 as a dotted curve relative to the location of the critical point and saturation phase boundary.

3.5. Computer-program verification

Tables 4 and 5 are provided to assist the user in computer-program verification. The viscosity calculations are based on the tabulated temperatures and densities. Due to the numerical implementation of the critical enhancement, calculated values may differ by 0.000001 nm for ξ or 0.000001 $\mu\text{Pa s}$ for μ . In addition, care may need to be taken during coding if one is using molar units; one must use the value of the molar gas constant as specified in the EOS documentation.¹⁴

TABLE 4. Sample points for computer-program verification of the correlating equation (2) with $\mu_2 = 1$

T (K)	ρ (kg m ⁻³)	μ (μPa s)
298.15	0	10.035 938
298.15	1105	1 092.642 4
298.15	1130	1 088.362 6
373.15	1064	326.637 91
775.00	1	29.639 474
775.00	100	31.930 085
775.00	400	53.324 172

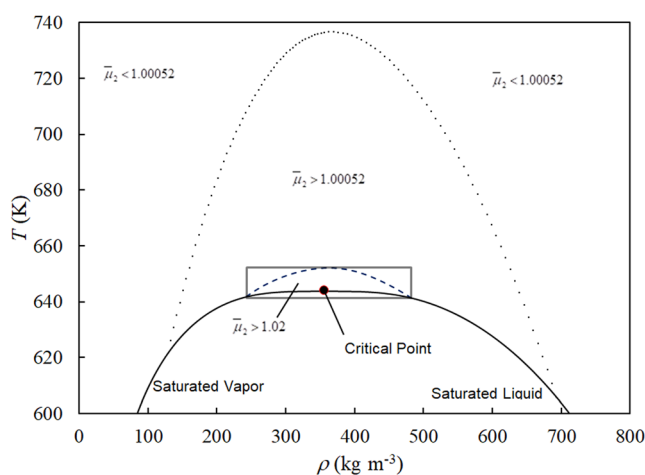


FIG. 9. Temperature and density regions where the viscosity enhancement $\bar{\mu}_2$ exceeds 1.000 52 (dotted curve) and 1.02 (dashed curve).

TABLE 5. Sample points for computer-program verification of the correlating equation (2) in the region near the critical point

T (K)	ρ (kg m ⁻³)	ξ (nm)	$\bar{\mu}_2$	μ (μPa s)
644.101	145	0.358 588	1.000 359	26.640 959
644.101	245	1.612 131	1.014 771	32.119 967
644.101	295	5.034 204	1.050 059	36.828 275
644.101	345	15.100 541	1.106 000	43.225 017
644.101	395	9.678 685	1.080 915	47.193 530
644.101	445	2.903 436	1.030 066	50.241 640

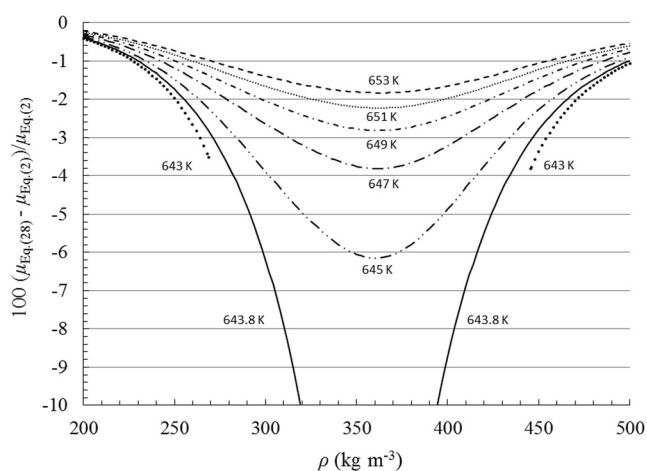
3.6. Recommendation for industrial applications

For industrial applications where greater computing speed is needed, it is recommended that the viscosity be calculated from

$$\bar{\mu} = \bar{\mu}_b = \bar{\mu}_0(\bar{T}) \times \bar{\mu}_1(\bar{T}, \bar{\rho}), \quad (27)$$

with $\bar{\mu}_0(\bar{T})$ as specified in Sec. 3.1 and with $\bar{\mu}_1(\bar{T}, \bar{\rho})$ as specified in Sec. 3.2. The EOS of Herrig *et al.*¹⁴ should be used to determine the density for use in Eq. (27) when the state point is defined by the temperature and pressure or other state variables. Physically, this means that for industrial applications, the critical viscosity enhancement can be neglected and the viscosity μ can be identified with the background viscosity μ_b , defined by Eq. (13), everywhere including in the near-critical region.

With this recommended industrial formulation for the viscosity of D₂O, the error introduced is smaller than the uncertainty of the scientific viscosity formulation given by Eq. (2), provided that the point is within the range of validity of the EOS, except for points close to and inside the near-critical region described by Eq. (25). Deviations between the viscosities calculated from the industrial viscosity formulation and the complete scientific viscosity formulation are shown in Fig. 10. The region of densities and temperatures where the

**FIG. 10.** Deviations along selected isotherms between the full model [Eq. (2)] and the simplified model for industrial applications [Eq. (27)].

deviations exceed 2% is very small and may in practice be ignored for industrial applications.

3.7. Liquid D₂O at 0.1 MPa

It is useful to have a simple correlation for the viscosity of liquid D₂O at atmospheric pressure (0.1 MPa) with uncertainties no greater than that of the full formulation developed as Eq. (2). A simplified equation was developed by fitting the primary experimental data at atmospheric pressure to the form

$$\bar{\mu} = \sum_{i=1}^4 a_i \bar{T}^{b_i}, \quad (28)$$

where the coefficients a_i and exponents b_i are given in Table 6. Equation (28) may be used over the range

$$242.16 \text{ K} \leq T \leq 374.54 \text{ K}. \quad (29)$$

Some points within this range are in the metastable liquid region, and as discussed earlier, the densities for the metastable region used in developing Eq. (2) were obtained from the work of Duška *et al.*⁶¹ rather than from the EOS of Herrig *et al.*¹⁴ The uncertainty for Eq. (28) is 1% for the stable liquid region and 3.5% for the metastable supercooled liquid at temperatures from the triple point (276.969 K)

TABLE 6. Coefficients a_i and exponents b_i in Eq. (28) for the viscosity of liquid D₂O at 0.1 MPa

i	a_i	b_i
1	96.892 3	-1.005 87
2	4.300 72	-6.565 94
3	$9.026\,97 \times 10^{-4}$	-16.069 1
4	$1.080\,54 \times 10^{-14}$	-42.655 1

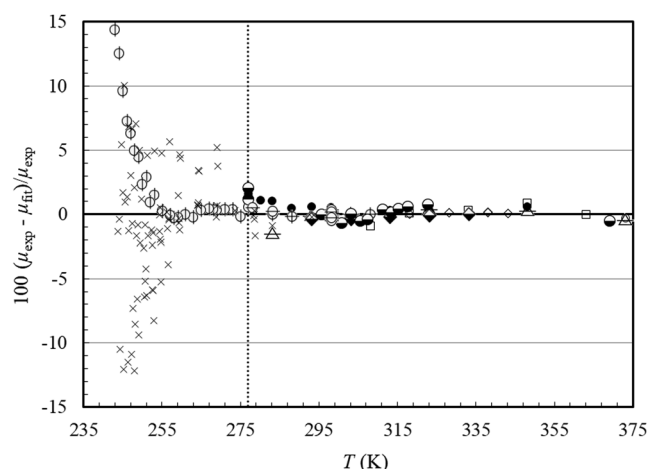
**FIG. 11.** Deviations of the primary data at 0.1 MPa from Eq. (28): Harlow⁴⁴ (△), Agayev and Usibova⁴³ (●), Selecki *et al.*⁴² (□), Agayev *et al.*⁴⁰ (○), Millero *et al.*⁴¹ (◇), Kellomaki³⁴ (⊕), Osipov *et al.*³³ (⊖), Gonçalves²⁸ (◆), Agayev²⁷ (⊙), Agayev²⁴ (⊗), Harris and Woolf²³ (⊖), and Issenmann and Caupin²² (×).

TABLE 7. Summary of critical region constants

Constant	Value
x_μ	0.068
q_C^{-1}	1.9 nm
q_D^{-1}	0.4 nm
ν	0.630
γ	1.239
ξ_0	0.13 nm
Γ_0	0.06
\bar{T}_R	1.5

down to 260 K and 7% for 250–260 K, rising to 13% at 242 K. When using the full formulation [Eq. (2)], if the density is computed from the EOS of Herrig *et al.*,¹⁴ the uncertainties are the same except for the very lowest temperatures from 244 to 250 K, where the uncertainty reaches 14%. Figure 11 shows the deviations of Eq. (28) as a function of temperature from all primary data at 0.1 MPa. The vertical dotted line denotes the location of the triple-point temperature. In the supplementary material of their work on supercooled water, Dehaoui *et al.*⁹⁹ stated that the large differences between their work and the work of Osipov *et al.*³³ are due to a bias of the Poiseuille flow experiments due to electro-osmotic effects, and this also would explain

TABLE 8. Summary of comparisons of Eq. (2) with experimental data and the previous 2007 IAPWS formulation for the viscosity

First author	Uncertainty (%) ^a	Number of data	Present work				Previous IAPWS formulation ¹²			
			AAD	AVG	STDEV	MAX	AAD	AVG	STDEV	MAX
Primary data										
Issenmann ²²	2–7	78	3.68	−0.70	4.70	12.93	4.03	−0.96	4.89	12.77
Harris ²³	1	128	0.58	−0.38	0.68	−2.31	8.71	−8.71	14.17	−64.83
Agayev ²⁴	1.2	182	0.59	0.18	0.74	−3.66	3.92	−3.76	4.26	−20.22
Rivkin ²⁵	1	57	2.20	1.39	2.88	10.91	5.73	5.65	4.12	18.17
Kestin ²⁶	0.2	72	0.47	−0.44	0.34	−1.43	0.64	−0.62	0.54	−2.01
Agayev ²⁷	0.5–1.5	172	1.98	−1.38	2.38	−13.02	1.15	0.60	1.39	−7.07
Goncalves ²⁸	0.1	6	0.14	0.07	0.14	0.24	0.18	−0.18	0.19	−0.51
Rivkin ²⁹	1	71	0.68	0.09	0.96	3.70	3.71	3.71	1.54	11.44
Abe ³⁰	1.5	40	2.23	−2.23	1.40	−5.80	0.72	−0.51	0.72	−1.85
Kinoshita ³¹	0.5	50	1.18	−0.26	1.67	−5.99	0.95	−0.10	1.18	2.85
Osipov ³³	1.5–3	26	4.28	2.93	5.76	17.08	5.20	2.74	6.81	19.00
Kellomaki ³⁴	0.1	6	0.38	0.38	0.05	0.43	0.21	0.07	0.21	−0.33
Rivkin ^{25,36}	1	50	0.64	−0.46	0.79	−2.21	0.83	0.05	1.15	4.26
Rivkin ³⁸	1	69	0.36	−0.14	0.97	4.22	0.80	0.37	1.55	8.40
Timrot ³⁹	0.35	15	0.28	−0.20	0.30	−0.51	0.40	0.40	0.22	0.96
Agayev ⁴⁰	1	157	0.80	0.49	0.95	3.91	0.98	0.29	1.25	4.47
Millero ⁴¹	na	28	0.17	0.16	0.12	0.35	0.24	−0.19	0.26	−0.77
Selecki ⁴²	0.8	6	0.47	0.28	0.48	0.92	0.39	−0.10	0.47	−0.71
Agayev ⁴³	0.5	257	0.53	0.23	0.66	4.56	0.53	0.05	0.68	4.23
Harlow ⁴⁴	1.4	96	0.747	−0.16	1.02	−4.41	6.72	2.07	12.07	42.70
Bonilla ⁴⁵	0.3	15	1.31	−1.14	1.19	−2.88	1.09	−0.70	1.10	−2.29
Secondary data										
Frost ⁴⁶	4	13 ^b	4.88	1.05	5.73	12.75	7.88	−4.77	8.061	−18.04
DeFries ⁴⁷	2	36	3.40	−3.24	2.56	−10.38	33.66	−33.66	28.17	−102.43
Lee ⁵⁰	2	55	1.97	−1.71	1.93	−7.69	1.93	−0.88	2.52	−9.85
Timrot ⁵¹	0.5	24	3.39	3.39	1.84	9.79	3.24	3.22	2.02	10.28
Heike ⁵²	3	12	0.95	0.20	1.47	4.49	1.21	−0.09	1.80	5.04
Hardy ^{53,54}	0.25	11	0.23	0.16	0.24	0.64	0.59	−0.48	0.44	−0.98
Lemonde ⁵⁵	na	17	2.10	0.60	2.95	8.68	2.18	0.04	2.82	7.90
Jones ⁵⁶	na	1	0.42	0.42	na	0.42	0.35	0.35	na	0.35
Baker ⁵⁷	na	1	12.55	12.55	na	12.55	11.09	11.09	na	11.09
Taylor ⁵⁸	na	1	1.12	1.12	na	1.12	1.02	1.02	na	1.02
Lewis ⁵⁹	0.5	7	0.80	0.63	0.65	1.39	0.60	0.25	0.64	1.02
Selwood ⁶⁰	na	1	13.96	13.96	na	13.96	12.18	12.18	na	12.18

^ana: Not available.^bExcludes three points that exceed the maximum pressure of the EOS (1200 MPa).

the large differences between the work of Issenmann and Caupin²² and that of Osipov *et al.*³³

4. Evaluation

In summary, the recommended formulation for the viscosity is given by Eq. (2),

$$\bar{\mu} = \bar{\mu}_0(\bar{T}) \times \bar{\mu}_1(\bar{T}, \bar{\rho}) \times \bar{\mu}_2(\bar{T}, \bar{\rho}). \quad (30)$$

The function $\bar{\mu}_0(\bar{T})$ is given by Eq. (3), and the function $\bar{\mu}_1(\bar{T}, \bar{\rho})$ is given by Eq. (4) with coefficients in Table 3. The function $\bar{\mu}_2(\bar{T}, \bar{\rho})$ is given by Eq. (14) as a function of $Y(\xi)$ defined by Eq. (21) for $0 \leq \xi \leq 0.030\,218\,066\,92$ nm and by Eq. (15) for $\xi > 0.030\,218\,066\,92$ nm. For convenience, the critical region constants are summarized in Table 7.

4.1. Comparisons with experimental data and the 2007 IAPWS formulation for viscosity

In order to evaluate performance, we compared the results of the new formulation [Eq. (2)], and also the 2007 IAPWS formulation¹² for the viscosity, with the experimental database. Comparisons with all points in the experimental database are presented in Table 8, which gives the average percent deviation, the average absolute percent deviation (AAD), the standard deviation, and the maximum percent deviation of each data source. Some points are extrapolations of the 2007 IAPWS formulation¹² because they are outside of its recommended range of temperatures and densities. All densities were calculated with the new EOS of Herrig *et al.*,¹⁴ with the exception of points in the supercooled liquid region below the triple-point temperature at atmospheric pressure where the densities were obtained from Duška *et al.*⁶¹ We define the percent deviation as $P = 100 * (\mu_{\text{exp}} - \mu_{\text{fit}})/\mu_{\text{exp}}$, where μ_{exp} is the experimental value of the viscosity and μ_{fit} is the value calculated from the present formulation [Eq. (2)]. The AAD is found with the expression

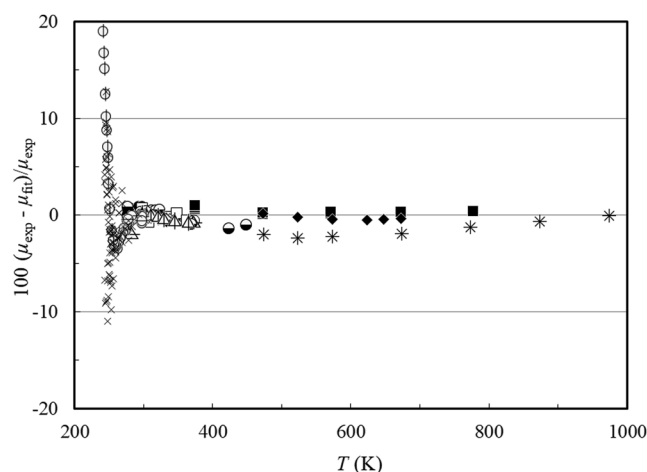


FIG. 13. Percentage deviations of the primary experimental data from the 2007 IAPWS formulation as a function of temperature for pressures below 0.102 MPa: Bonilla *et al.*⁴⁵ (recalculated) (*), Harlow⁴⁴ (Δ), Agayev and Usibova⁴³ (\bullet), Selecki *et al.*⁴² (\square), Agayev *et al.*⁴⁰ (\circ), Millero *et al.*⁴¹ (\diamond), Timrot *et al.*³⁹ (\blacksquare), Kellomaki³⁴ (\oplus), Osipov *et al.*³³ (Φ), Abe *et al.*³⁰ (\blacklozenge), Agayev²⁷ (\ominus), Gonçalves²⁸ (\blacklozenge), Kestin *et al.*²⁶ (Δ), Agayev²⁴ (\ominus), Harris and Woolf²³ (\ominus), and Issenmann and Caupin²² (\times).

$\text{AAD} = (\sum |P|)/n$, where the summation is over all n points; the average percent deviation is $\text{AVG} = (\sum P)/n$, and the standard deviation is $\text{STDEV} = ([n \sum P^2 - (\sum P)^2]/n^2)^{1/2}$. As indicated in Table 8, the results of the new formulation and the 2007 IAPWS formulation for the viscosity for the data sources that were used in the earlier IAPWS formulation are in most cases comparable, with the most significant differences observed mainly in areas where the earlier formulation was not applicable, such as pressures above 100 MPa.

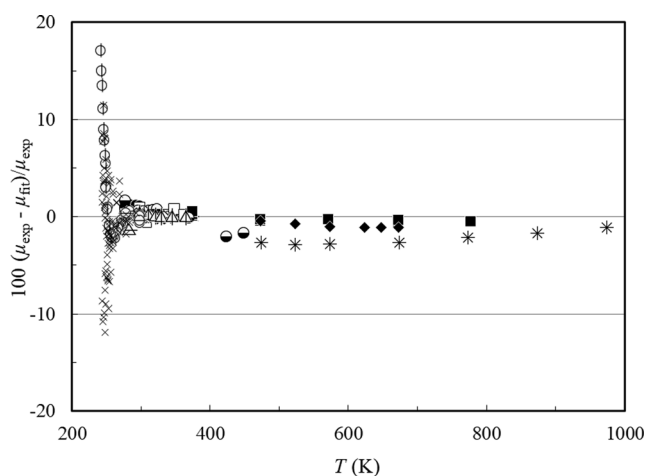


FIG. 12. Percentage deviations of the primary experimental data from the present formulation as a function of temperature for pressures below 0.102 MPa: Bonilla *et al.*⁴⁵ (recalculated) (*), Harlow⁴⁴ (Δ), Agayev and Usibova⁴³ (\bullet), Selecki *et al.*⁴² (\square), Agayev *et al.*⁴⁰ (\circ), Millero *et al.*⁴¹ (\diamond), Timrot *et al.*³⁹ (\blacksquare), Kellomaki³⁴ (\oplus), Osipov *et al.*³³ (Φ), Abe *et al.*³⁰ (\blacklozenge), Agayev²⁷ (\ominus), Gonçalves²⁸ (\blacklozenge), Kestin *et al.*²⁶ (Δ), Agayev²⁴ (\ominus), Harris and Woolf²³ (\ominus), and Issenmann and Caupin²² (\times).

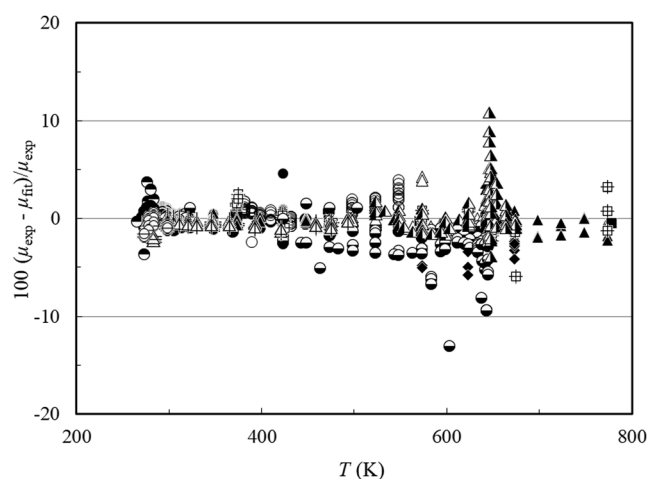


FIG. 14. Percentage deviations of the primary experimental data from the present formulation as a function of temperature for pressures between 0.102 and 100 MPa: Harlow⁴⁴ (Δ), Agayev and Usibova⁴³ (\bullet), Agayev *et al.*⁴⁰ (\circ), Rivkin *et al.*³⁸ (Δ), Rivkin *et al.*²⁵ (\blacktriangle), Timrot *et al.*³⁹ (\blacksquare), Abe *et al.*³⁰ (\blacklozenge), Kinoshita *et al.*³¹ (\oplus), Agayev²⁷ (\ominus), Rivkin *et al.*²⁹ (Δ), Kestin *et al.*²⁶ (Δ), Rivkin and Romashin²⁵ (\blacktriangle), Agayev²⁴ (\ominus), and Harris and Woolf²³ (\ominus).

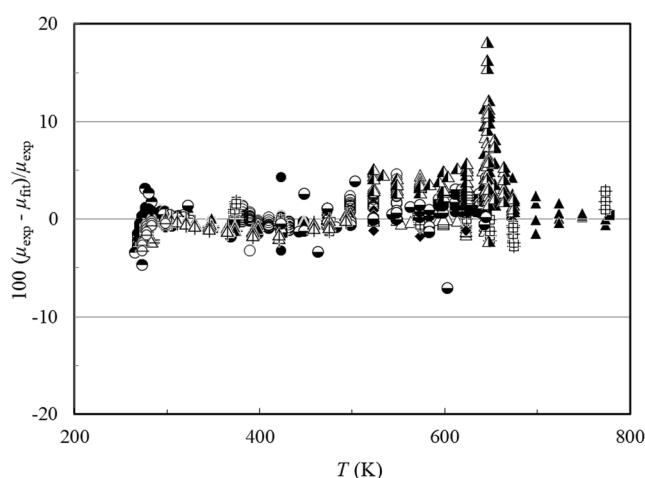


FIG. 15. Percentage deviations of the primary experimental data from the 2007 IAPWS formulation as a function of temperature for pressures between 0.102 and 100 MPa: Harlow⁴⁴ (Δ), Agayev and Usibova⁴³ (\bullet), Agayev *et al.*⁴⁰ (\circ), Rivkin *et al.*³⁸ (Δ), Rivkin *et al.*²⁵ (\blacktriangle), Timrot *et al.*³⁹ (\blacksquare), Abe *et al.*³⁰ (\blacklozenge), Kinoshita *et al.*³¹ (\boxplus), Agayev²⁷ (\ominus), Rivkin *et al.*²⁹ (\blacktriangle), Kestin *et al.*²⁶ (\blacktriangle), Rivkin and Romashin²⁵ (\blacktriangle), Agayev²⁴ (\bullet), and Harris and Woolf²³ (\ominus).

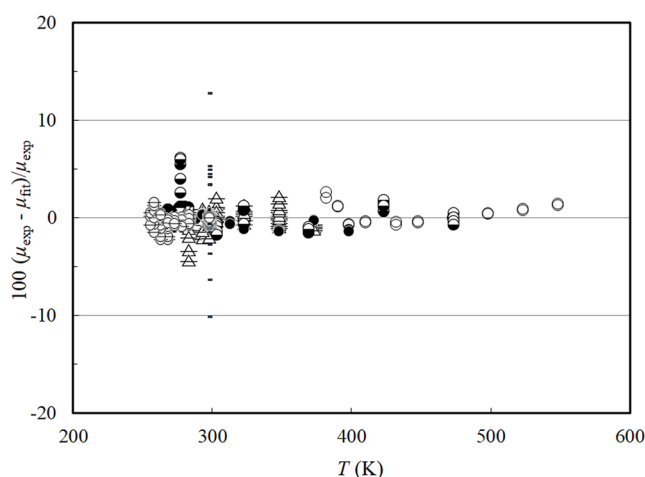


FIG. 16. Percentage deviations of the primary experimental data from the present formulation as a function of temperature for pressures above 100 MPa: Harlow⁴⁴ (Δ), Agayev and Usibova⁴³ (\bullet), Agayev *et al.*⁴⁰ (\circ), Agayev²⁷ (\ominus), Agayev²⁴ (\bullet), Harris and Woolf²³ (\ominus), and Frost and Glenzer⁴⁶ (\bullet).

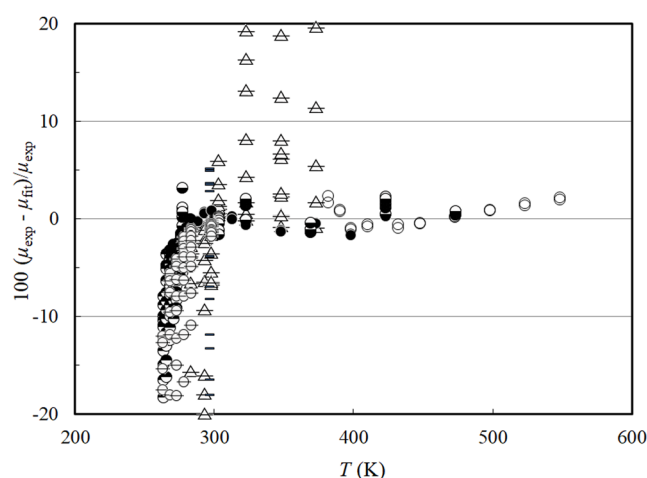


FIG. 17. Percentage deviations of the primary experimental data from the 2007 IAPWS formulation as a function of temperature for pressures above 100 MPa: Harlow⁴⁴ (Δ), Agayev and Usibova⁴³ (\bullet), Agayev *et al.*⁴⁰ (\circ), Agayev²⁷ (\ominus), Agayev²⁴ (\bullet), Harris and Woolf²³ (\ominus), and Frost and Glenzer⁴⁶ (\bullet).

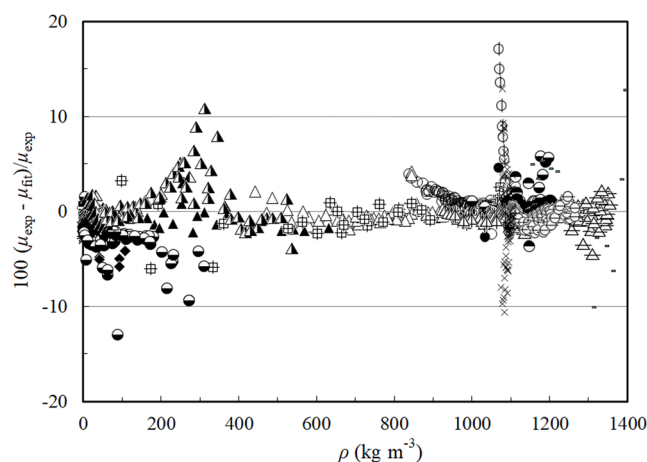


FIG. 18. Percentage deviations of the primary experimental data from the present formulation as a function of density: Bonilla *et al.*⁴⁵ (recalculated) (\ast), Harlow⁴⁴ (Δ), Agayev and Usibova⁴³ (\bullet), Selecki *et al.*⁴² (\square), Agayev *et al.*⁴⁰ (\circ), Millero *et al.*⁴¹ (\diamond), Rivkin *et al.*³⁸ (Δ), Rivkin *et al.*²⁵ (\blacktriangle), Timrot *et al.*³⁹ (\blacksquare), Kellomaki (\boxplus), Osipov *et al.*³³ (Φ), Abe *et al.*³⁰ (\blacklozenge), Kinoshita *et al.*³¹ (\boxplus), Agayev²⁷ (\ominus), Gonçalves²⁸ (\blacklozenge), Rivkin *et al.*²⁹ (\blacktriangle), Kestin *et al.*²⁶ (\blacktriangle), Rivkin and Romashin²⁵ (\blacktriangle), Agayev²⁴ (\bullet), Harris and Woolf²³ (\ominus), Isenmann and Caupin²² (\times), and Frost and Glenzer⁴⁶ (\bullet).

Figures 12–17 show the percent deviations of the present model and the 2007 IAPWS formulation with the primary experimental data as a function of temperature for three different pressure ranges, while Figs. 18 and 19 display the same deviations as a function of density, and Figs. 20–25 show deviations as a function of pressure for three different ranges of temperature. In addition, although not in the primary data and not used in the development of the formulation, comparisons with the data of Frost and Glenzer⁴⁶ are also indicated in the figures. Three points from Ref. 46 that exceed the upper limit of

the EOS (1200 MPa) are not included in the comparisons for either the current model or the 2007 IAPWS formulation. In the figures associated with the 2007 IAPWS formulation, some very high-pressure points are out of the range of the figures. It should be noted that the stated range of applicability for the 2007 IAPWS formulation¹² is $0 \text{ MPa} \leq p \leq 100 \text{ MPa}$ and $277 \text{ K} \leq T \leq 775 \text{ K}$, but it was stated that reasonable extrapolation could be expected up to 200 MPa.⁹ We note that the 2007 IAPWS formulation was not developed for, or intended for, use at pressures above 200 MPa; it can have very

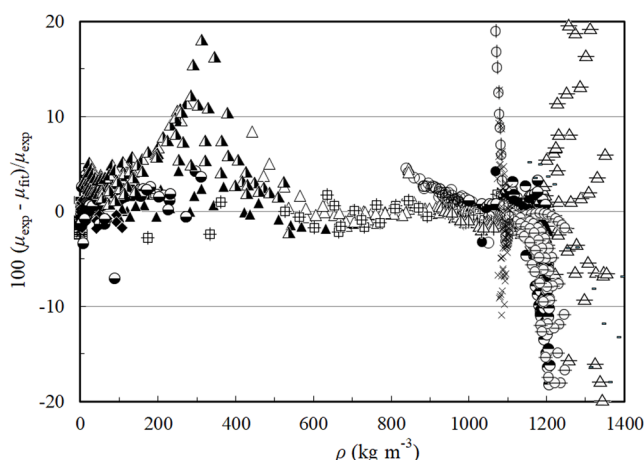


FIG. 19. Percentage deviations of the primary experimental data from the 2007 IAPWS formulation as a function of density. Bonilla *et al.*⁴⁵ (recalculated) (*), Harlow⁴⁴ (△), Agayev and Usibova⁴³ (●), Selecki *et al.*⁴² (□), Agayev *et al.*⁴⁰ (○), Millero *et al.*⁴¹ (◇), Rivkin *et al.*³⁸ (△), Rivkin *et al.*²⁵ (▲), Timrot *et al.*³⁹ (■), Kellomaki³⁴ (⊕), Osipov *et al.*³³ (Φ), Abe *et al.*³⁰ (◆), Kinoshita *et al.*³¹ (⊞), Agayev²⁷ (●), Gonçalves²⁸ (◇), Rivkin *et al.*²⁹ (▲), Kestin *et al.*²⁶ (△), Rivkin and Romashin²⁵ (▲), Agayev²⁴ (●), Harris and Woolf²³ (⊖), Issenmann and Caupin²² (×), and Frost and Glenzer⁴⁶ (≡).

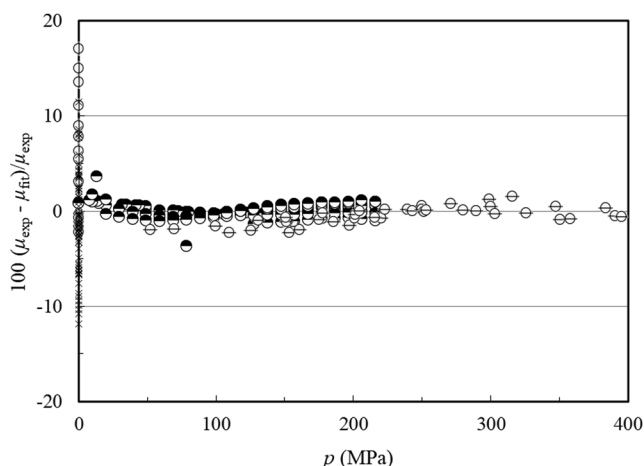


FIG. 20. Percentage deviations of the primary experimental data from the present formulation as a function of pressure for temperatures below 276.97 K: Osipov *et al.*³³ (Φ), Agayev²⁴ (●), Harris and Woolf²³ (⊖), and Issenmann and Caupin²² (×).

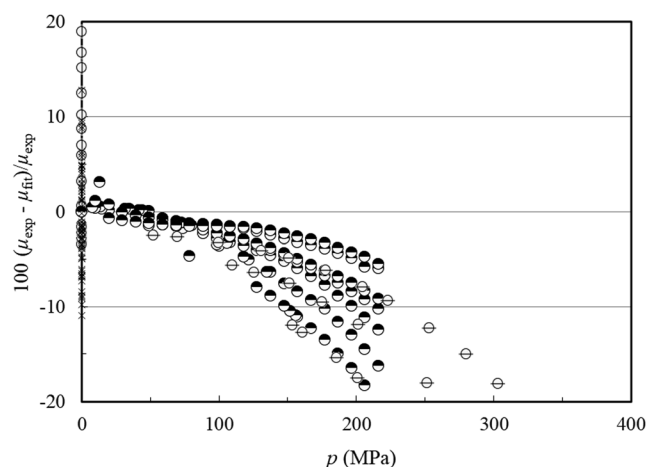


FIG. 21. Percentage deviations of the primary experimental data from the 2007 IAPWS formulation as a function of pressure for temperatures below 276.97 K: Osipov *et al.*³³ (Φ), Agayev²⁴ (●), Harris and Woolf²³ (⊖), and Issenmann and Caupin²² (×).

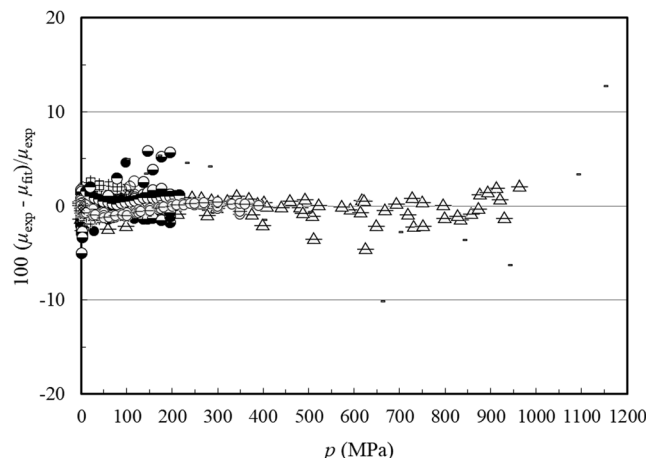


FIG. 22. Percentage deviations of the primary experimental data from the present formulation as a function of pressure for temperatures between 277 and 500 K: Bonilla *et al.*⁴⁵ (recalculated) (*), Harlow⁴⁴ (△), Agayev and Usibova⁴³ (●), Selecki *et al.*⁴² (□), Agayev *et al.*⁴⁰ (○), Millero *et al.*⁴¹ (◇), Rivkin *et al.*³⁸ (△), Rivkin *et al.*²⁵ (▲), Timrot *et al.*³⁹ (■), Kellomaki³⁴ (⊕), Osipov *et al.*³³ (Φ), Abe *et al.*³⁰ (◆), Kinoshita *et al.*³¹ (⊞), Agayev²⁷ (●), Gonçalves²⁸ (◇), Kestin *et al.*²⁶ (△), Agayev²⁴ (●), Harris and Woolf²³ (⊖), Issenmann and Caupin²² (×), and Frost and Glenzer⁴⁶ (≡).

large deviations, reaching almost 80%, when extrapolated to pressures approaching 1000 MPa. It is not appropriate to make comparisons outside of the intended range of a correlation; we show these comparisons primarily to demonstrate the dangers of using an empirical correlation outside of its intended range.

The primary region where there are significant differences in the performance of the previous IAPWS formulation for the

viscosity and this work are for the liquid at very high pressures, demonstrated by the deviations shown for the datasets of Harris and Woolf,²³ Harlow,⁴⁴ and Agayev.^{24,27} As already mentioned, the 2007 IAPWS formulation is recommended for use only up to 100 MPa; this was because the formulation is in terms of T and ρ and, hence, was tied to the EOS of Hill *et al.*⁸ that was limited to 100 MPa. As noted by Matsunaga and Nagashima,⁹ their formulation may be extended to 200

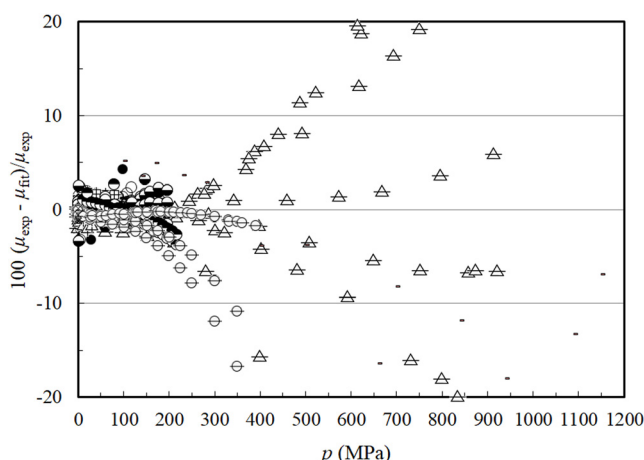


FIG. 23. Percentage deviations of the primary experimental data from the 2007 IAPWS formulation as a function of pressure for temperatures between 277 K and 500 K: Bonilla *et al.*⁴⁵ (recalculated) (*), Harlow⁴⁴ (△), Agayev and Usibova⁴³ (●), Selecki *et al.*⁴² (□), Agayev *et al.*⁴⁰ (○), Millero *et al.*⁴¹ (◇), Rivkin *et al.*³⁸ (△), Rivkin *et al.*²⁵ (▲), Timrot *et al.*³⁹ (■), Kellomaki³⁴ (⊕), Osipov *et al.*³³ (⊖), Abe *et al.*³⁰ (◆), Kinoshita *et al.*³¹ (⊞), Agayev²⁷ (⊙), Gonçalves²⁸ (◇), Kestin *et al.*²⁶ (△), Agayev²⁴ (●), Harris and Woolf²³ (⊖), Issenmann and Caupin²² (×), and Frost and Glenzer⁴⁶ (=).

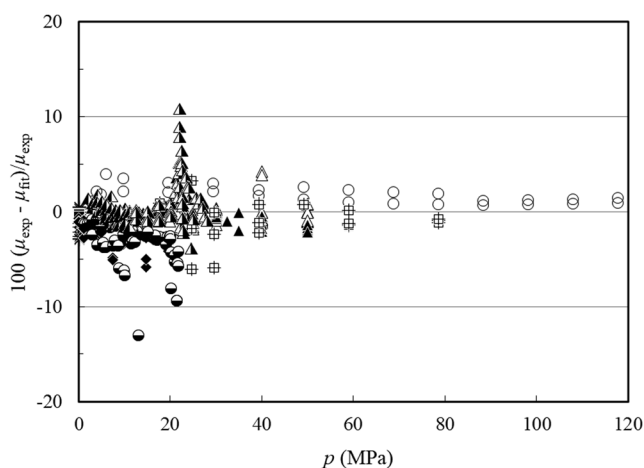


FIG. 24. Percentage deviations of the primary experimental data from the present formulation as a function of pressure for temperatures above 500 K: Bonilla *et al.*⁴⁵ (recalculated) (*), Agayev *et al.*⁴⁰ (○), Rivkin *et al.*³⁸ (△), Rivkin *et al.*²⁵ (▲), Timrot *et al.*³⁹ (■), Abe *et al.*³⁰ (◆), Kinoshita *et al.*³¹ (⊞), Agayev²⁷ (⊙), Rivkin *et al.*²⁹ (▲), and Rivkin and Romashin²⁵ (▲).

MPa for temperatures between the triple point and 473 K; above 200 MPa, the deviations increase significantly. The data of Harlow cover the temperature range from 283 to 373 K and extend to 964 MPa. The present formulation represents this dataset to about 2.5% over the entire pressure range to almost 1000 MPa. The more recent data of Harris and Woolf extend from 256 to 298 K at pressures up to 395 MPa, and the authors give an estimated experimental uncertainty of 1%. The present formulation, as indicated in Table 8, represents these data to within about 1.4%, slightly more than the experimental uncertainty. The data of

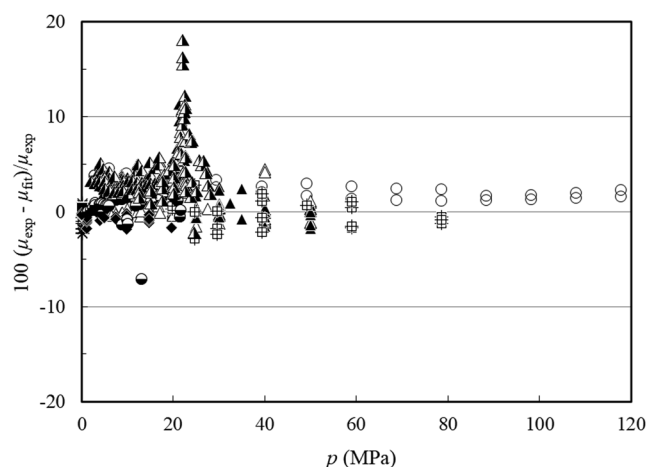


FIG. 25. Percentage deviations of the primary experimental data from the 2007 IAPWS formulation as a function of pressure for temperatures above 500 K: Bonilla *et al.*⁴⁵ (recalculated) (*), Agayev *et al.*⁴⁰ (○), Rivkin *et al.*³⁸ (△), Rivkin *et al.*²⁵ (▲), Timrot *et al.*³⁹ (■), Abe *et al.*³⁰ (◆), Kinoshita *et al.*³¹ (⊞), Agayev²⁷ (⊙), Rivkin *et al.*²⁹ (▲), and Rivkin and Romashin²⁵ (▲).

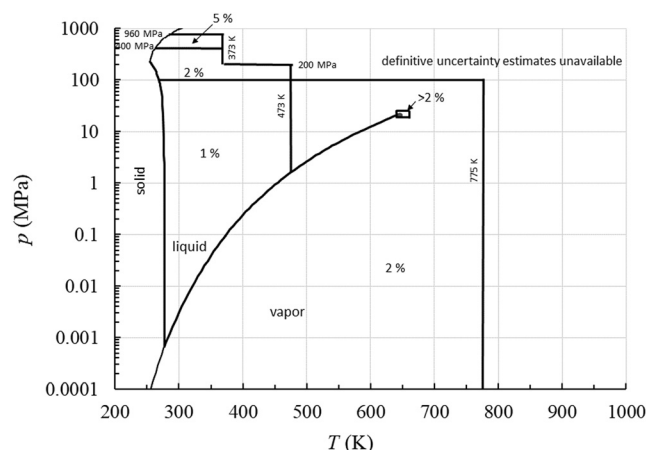


FIG. 26. Expanded uncertainties of the present formulation for the viscosity of heavy water.

Agayev²⁴ covering 263–283 K near the freezing curve at pressures up to 216 MPa are represented to within 1.6%, which is only slightly more than their estimated uncertainty of 1.2%. Deviations for the other Agayev²⁷ dataset, containing data at pressures up to 196 MPa, have larger deviations but generally are within about 4%.

4.2. Range and uncertainty estimates for the formulation

The domain of validity of the formulation encompasses all thermodynamically stable fluid states in the following ranges of pressure p and temperature T :

$$\begin{array}{ll} 0 < p \leq p_t & \text{and } T_t \leq T \leq 775 \text{ K,} \\ p_t \leq p \leq 100 \text{ MPa} & \text{and } T_m(p) \leq T \leq 775 \text{ K,} \\ 100 \text{ MPa} < p \leq 200 \text{ MPa} & \text{and } T_m(p) \leq T \leq 473 \text{ K,} \\ 200 \text{ MPa} < p \leq 960 \text{ MPa} & \text{and } T_m(p) \leq T \leq 373 \text{ K.} \end{array} \quad (31)$$

In Eq. (31), T_m is the pressure-dependent melting temperature,¹⁴ $T_t = 276.969 \text{ K}$ is the triple-point temperature,¹⁴ and $p_t = 0.661 59 \text{ kPa}$ is the triple-point pressure.¹⁴ The density from the EOS of Herrig *et al.*¹⁴ should be used to determine the densities used as input to Eq. (2), when the state point under consideration is defined by pressure and temperature or by other thermodynamic variables instead of density and temperature.

In addition, as mentioned in Sec. 3.1, the dilute-gas component of Eq. (2) behaves in a physically reasonable manner up to at least 2500 K. Furthermore, for vapor states at temperatures below the triple-point temperature of 276.969 K and pressures less than or equal to the sublimation pressure, the viscosity calculation is dominated by the dilute-gas term, and this behaves in a physically reasonable manner down to at least 250 K. For stable fluid states outside the range of validity of Eq. (31) but within the range of validity of the Revised Release on the IAPWS Formulation 2017 for the Thermodynamic Properties of Heavy Water,¹⁵ the extrapolation behavior of Eq. (2) is physically reasonable. The current formulation may also be used for extrapolation into the metastable subcooled liquid at atmospheric pressure down to 242 K. For calculating density in the metastable liquid below the triple point, we used the method of Duška *et al.*⁶¹

For the development of the estimates of uncertainty, we relied upon comparisons with the previous IAPWS formulation for the viscosity¹² and with a subset of the experimental database used to develop the correlation. The subset contained the data with the lowest uncertainties for specific regions in the phase diagram. The relative uncertainties in this formulation are summarized in Fig. 26. The uncertainty estimates can be considered as estimates of an expanded uncertainty with a coverage factor of 2.

5. Conclusions

The international task group, comprising members affiliated with IAPWS and the IUPAC transport properties committee (now established as the International Association for Transport Properties), has completed its examination of the data, theory, and models most appropriate for describing the viscosity of heavy water over broad ranges of temperature and pressure. The resulting equation (2), with subsidiary equations and the accompanying tables of coefficients and parameters, should allow calculation of the viscosity of heavy water for most purposes according to international consensus and within uncertainty bounds achievable with current information. As evidenced by Fig. 26, there still are regions where the availability of new experimental data with low uncertainties could lead to improvements in future representations of the viscosity surface of D₂O. Furthermore, improvements in theory may better elucidate the high-temperature extrapolation behavior.

The form of Eq. (2) and the general forms of the constituent factors are similar to those established in the earlier standard formulation¹² but now include the term $\bar{\mu}_2$ that provides a theoretical description of the critical region. The new formulation also allows calculations in a broader range of state variables, considers an expanded set of experimental data, incorporates advances in the

calculation of the zero-density viscosity by Hellmann and Bich,¹⁶ can be used in the metastable supercooled region down to 242 K, and is consistent with the recent consensus formulation for the thermodynamic properties of heavy water. The comparisons of Sec. 4 provide support for the uncertainty estimates over the full range of applicability of the formulation.

In addition, the viscosity is needed for the development of a correlation for the thermal conductivity, where it is used in the terms involving the critical enhancement of the thermal conductivity. A new thermal conductivity formulation for heavy water has been developed and is currently being evaluated by IAPWS.

The recently adopted IAPWS Release on the Viscosity of Heavy Water¹⁸ provides a concise description of the correlating equations for potential users. This paper provides a detailed explanation of the formulation.

Acknowledgments

We thank M. Duška (Institute of Thermomechanics of the CAS, Czech Republic) for providing density values for the data in the metastable supercooled region and B. Issenmann and F. Caupin (University of Lyon) for providing viscosity data in the metastable supercooled region prior to publication. We also thank A. H. Harvey (NIST, Boulder), A. Nagashima (Keio University), R. Hellmann (Helmut-Schmidt-Universität), K. Meier (Helmut-Schmidt-Universität), and A. Blahut (Czech Academy of Sciences) for many helpful suggestions and discussions.

6. Data Availability

Data sharing is not applicable to this article as no new data were created or analyzed in this study.

7. References

- ¹D. Kramer, *Phys. Today* **74**(1), 23 (2021).
- ²I. Kirshenbaum, *Physical Properties and Analysis of Heavy Water* (McGraw-Hill, New York, 1951).
- ³Y. Z. Kazavchinskii, O. M. Kessel'man, V. A. Kirillin, S. L. Rivkin, A. E. Sheindlin, E. E. Shpil'rain, V. V. Sychev, and D. L. Timrot, *Tyazhelyaya Voda: Teplofizicheskoe Svoistvo* (Gosenergoizdat, Moscow, 1963).
- ⁴J. T. R. Watson, An Assessment of the Values of the Viscosity of D₂O at Zero Density, Report to WG-II, IAPS, National Engineering Laboratory, East Kilbridge, Glasgow, 1979.
- ⁵A. Nagashima and N. Matsunaga, in *Proceedings of the 9th International Conference on the Properties of Steam, Munich*, edited by J. Straub and K. Scheffler (Pergamon, Oxford, 1980), pp. 344–353.
- ⁶M. Ikeda, Y. Kageyama, and A. Nagashima, *Bull. JSME* **20**, 1942 (1977).
- ⁷R. Pollak, *Brennst.-Waerme-Kraft* **27**, 210 (1975).
- ⁸P. G. Hill, R. D. C. MacMillan, and V. Lee, *J. Phys. Chem. Ref. Data* **11**, 1 (1982).
- ⁹N. Matsunaga and A. Nagashima, *J. Phys. Chem. Ref. Data* **12**, 933 (1983).
- ¹⁰J. Kestin, J. V. Sengers, B. Kamgar-Parsi, and J. M. H. Levelt Sengers, *J. Phys. Chem. Ref. Data* **13**, 601 (1984).
- ¹¹Release on the IAPS formulation 1984 for the thermodynamic properties of heavy water substance, International Association for the Properties of Water and Steam, in *Proceedings of 12th International Conference on the Properties of Water and Steam*, edited by H. J. White, J. V. Sengers, D. B. Neumann, and J. C. Bellows (Begell House, New York, 1995), p. A88.
- ¹²See <http://www.iapws.org> for International Association for the Properties of Water and Steam, IAPWS R4-84(2007), Revised Release on Viscosity and Thermal Conductivity of Heavy Water Substance.

- ¹³A. A. Aleksandrov and A. B. Matveev, in *Proceedings of the 13th International Conference on the Properties of Water and Steam, Toronto, 1999*, edited by P. R. Tremaine, P. G. Hill, D. R. Irish, and P. V. Balakrishnan (NRC Research Press, Ottawa, 2000), pp. 80–87.
- ¹⁴S. Herrig, M. Thol, A. H. Harvey, and E. W. Lemmon, *J. Phys. Chem. Ref. Data* **47**, 043102 (2018).
- ¹⁵See <http://www.iapws.org/relguide/Heavy.html> for International Association for the Properties of Water and Steam, IAPWS R16-17 (2018), Revised Release on the IAPWS Formulation 2017 for the Thermodynamic Properties of Heavy Water, 2018.
- ¹⁶R. Hellmann and E. Bich, *Mol. Phys.* **115**, 1057 (2017).
- ¹⁷See <http://www.iapws.org/relguide/fundam.pdf> for International Association for the Properties of Water and Steam, IAPWS G5-01(2020), Guideline on the Use of Fundamental Physical Constants and Basic Constants of Water.
- ¹⁸See <http://www.iapws.org/relguide/D2Ovisc.html> for International Association for the Properties of Water and Steam, IAPWS R17-20, Release on the IAPWS Formulation 2020 for the Viscosity of Heavy Water, 2020.
- ¹⁹M. L. Huber, R. A. Perkins, A. Laesecke, D. G. Friend, J. V. Sengers, M. J. Assael, I. N. Metaxa, E. Vogel, R. Mareš, and K. Miyagawa, *J. Phys. Chem. Ref. Data* **38**, 101 (2009).
- ²⁰M. J. Assael, A. E. Kalyva, S. A. Monogenidou, M. L. Huber, R. A. Perkins, D. G. Friend, and E. F. May, *J. Phys. Chem. Ref. Data* **47**, 021501 (2018).
- ²¹M. J. Assael, V. K. Tsalmanis, N. K. Dalouti, D. Giakoumakis, and A. Nagashima, in *Proceedings of the 13th International Conference on the Properties of Water and Steam, Toronto, 1999*, edited by P. R. Tremaine, P. G. Hill, D. R. Irish, and P. V. Balakrishnan (NRC Research Press, Ottawa, 2000), pp. 72–79.
- ²²B. Issenmann and F. Caupin, Univ. of Lyon (personal communication to M. L. Huber, 2019).
- ²³K. R. Harris and L. A. Woolf, *J. Chem. Eng. Data* **49**, 1064 (2004).
- ²⁴N. A. Agayev, in *Proceedings of the 11th International Conference on the Properties of Water and Steam, Prague, 1989*, edited by M. Pichal and O. Šifner (Hemisphere Publishing Corporation, New York, 1990), pp. 148–153.
- ²⁵S. L. Rivkin and S. N. Romashin, in *Proceedings of the 10th International Conference on the Properties of Steam, Moscow, 1984*, edited by V. V. Sytchev and A. A. Aleksandrov (Mir Publishers, Moscow, 1986), Vol. 1, pp. 415–419.
- ²⁶J. Kestin, N. Imaishi, S. H. Nott, J. C. Nieuwoudt, and J. V. Sengers, *Physica A* **134**, 38 (1985).
- ²⁷N. A. Agayev, in *Proceedings of the 9th International Conference on the Properties of Steam, Munich, 1980*, edited by J. Straub and K. Scheffler (Pergamon, Oxford, 1980), pp. 362–374.
- ²⁸F. A. Gonçalves, in *Proceedings of the 9th International Conference on the Properties of Steam, Munich, 1980*, edited by J. Straub and K. Scheffler (Pergamon, Oxford, 1980), pp. 354–361.
- ²⁹S. Rivkin, A. Levin, L. Izrailevskii, K. Kharitonov, and S. Romashin, in *Proceedings of the 9th International Conference on the Properties of Steam, Munich, 1980*, edited by J. Straub and K. Scheffler (Pergamon, Oxford, 1980), pp. 375–381.
- ³⁰S. Abe, R. Fujioka, and A. Nagashima, *Bull. JSME* **21**, 142 (1978).
- ³¹H. Kinoshita, S. Abe, and A. Nagashima, *J. Chem. Eng. Data* **23**, 16 (1978).
- ³²H. Kinoshita, S. Abe, and A. Nagashima, in *Proceedings of the 8th International Conference on the Properties of Steam, Giens, 1974*, edited by P. Bury, H. Perdon, and B. Vodar (Editions Européennes Thermiques et Industries, Paris, 1975), pp. 167–177.
- ³³Y. A. Osipov, B. V. Zheleznyi, and N. F. Bondarenko, *Russ. J. Phys. Chem.* **51**, 1264 (1977).
- ³⁴A. Kellomäki, *Finn. Chem. Lett.* **2**, 51 (1975).
- ³⁵S. L. Rivkin, A. Y. Levin, L. B. Izrailevskii, and K. G. Kharitonov, in *Proceedings of the 8th International Conference on the Properties of Steam, Giens, 1974*, edited by P. Bury, H. Perdon, and B. Vodar (Editions Européennes Thermiques et Industries, Paris, 1975), pp. 153–162.
- ³⁶S. L. Rivkin, A. J. Levin, L. B. Izrailevskii, and K. G. Kharitonov, *Teploënergetika* **23**(11), 79 (1976).
- ³⁷S. L. Rivkin, A. J. Levin, L. B. Izrailevskii, K. G. Kharitonov, and V. N. Ptitsyna, *Teploënergetika* **24**(8), 65 (1977).
- ³⁸S. L. Rivkin, A. Y. Levin, L. B. Izrailevskii, and K. G. Kharitonov, *Teploënergetika* **21**(4), 69 (1974).
- ³⁹D. L. Timrot, M. A. Serednitskaya, and M. S. Bespalov, *Teploënergetika* **21**(3), 83 (1974).
- ⁴⁰N. A. Agayev, A. M. Kerimov, and A. Abaszade, *Sov. Atom. Energy* **30**, 655 (1971).
- ⁴¹F. J. Millero, R. Dexter, and E. Hoff, *J. Chem. Eng. Data* **16**, 85 (1971).
- ⁴²A. Selecki, B. Tyminski, and A. G. Chmielewski, *J. Chem. Eng. Data* **15**, 127 (1970).
- ⁴³N. A. Agayev and A. D. Usibova, *Dokl. Akad. Nauk SSSR* **180**, 334 (1968).
- ⁴⁴A. Harlow, Ph.D. Thesis, University of London, London, 1967.
- ⁴⁵C. F. Bonilla, J. Wang, and H. Weiner, *Trans. ASME* **78**, 1285 (1956).
- ⁴⁶M. Frost and S. H. Glenzer, *Appl. Phys. Lett.* **116**, 233701 (2020).
- ⁴⁷T. DeFries and J. Jonas, *J. Chem. Phys.* **66**, 5393 (1977).
- ⁴⁸A. I. Kudish and D. Wolf, *J. Phys. Chem.* **79**, 272 (1975).
- ⁴⁹D. Wolf and A. I. Kudish, *J. Phys. Chem.* **79**, 1481 (1975).
- ⁵⁰Y. Lee and J. Jonas, *J. Chem. Phys.* **57**, 4233 (1972).
- ⁵¹D. L. Timrot and K. F. Shuiskaya, *Sov. Atom. Energy* **7**, 458 (1959).
- ⁵²J. R. Heiks, M. K. Barnett, L. V. Jones, and E. Orban, *J. Phys. Chem.* **58**, 488 (1954).
- ⁵³R. C. Hardy and R. L. Cottingham, *J. Res. Natl. Bur. Stand.* **42**, 573 (1949).
- ⁵⁴R. C. Hardy and R. L. Cottingham, *J. Chem. Phys.* **17**, 509 (1949).
- ⁵⁵H. Lemonde and M. de Broglie, *C. R. Phys.* **212**, 81 (1941).
- ⁵⁶G. Jones and H. J. Fornwalt, *J. Chem. Phys.* **4**, 30 (1936).
- ⁵⁷W. N. Baker and V. K. La Mer, *J. Chem. Phys.* **3**, 406 (1935).
- ⁵⁸H. S. Taylor and P. W. Selwood, *J. Am. Chem. Soc.* **56**, 998 (1934).
- ⁵⁹G. N. Lewis and R. T. Macdonald, *J. Am. Chem. Soc.* **55**, 4730 (1933).
- ⁶⁰P. W. Selwood and A. A. Frost, *J. Am. Chem. Soc.* **55**, 4335 (1933).
- ⁶¹M. Duška, J. Hrubý, F. Caupin, and M. A. Anisimov, [arXiv:1708.04054v1](https://arxiv.org/abs/1708.04054v1) (2017).
- ⁶²A. Blahut, J. Hykl, P. Peukert, V. Vinš, and J. Hrubý, *J. Chem. Phys.* **151**, 034505 (2019).
- ⁶³M. L. Huber, R. A. Perkins, D. G. Friend, J. V. Sengers, M. J. Assael, I. N. Metaxa, K. Miyagawa, R. Hellmann, and E. Vogel, *J. Phys. Chem. Ref. Data* **41**, 033102 (2012).
- ⁶⁴V. Vasilenco, *Ann. Phys.* **11**, 137 (1945).
- ⁶⁵E. W. Lemmon and R. T. Jacobsen, *Int. J. Thermophys.* **25**, 21 (2004).
- ⁶⁶R. A. Svehla, “Estimated viscosities and thermal conductivities of gases at high temperatures,” NASA Technical Report No. TR-R-132, 1962.
- ⁶⁷R. S. Brokaw, NASA Technical Memorandum No. TM-X-52478, Statistical Mechanical Theories of Transport Properties, 1968.
- ⁶⁸J. T. R. Watson, R. S. Basu, and J. V. Sengers, *J. Phys. Chem. Ref. Data* **9**, 1255 (1980).
- ⁶⁹R. Krauss, J. Luettmer-Strathmann, J. V. Sengers, and K. Stephan, *Int. J. Thermophys.* **14**, 951 (1993).
- ⁷⁰S. Kirkpatrick, C. D. Gelatt, and M. P. Vecchi, *Science* **220**, 671 (1983).
- ⁷¹P. T. Boggs, R. H. Byrd, J. E. Rogers, and R. B. Schnabel, ODRPACK, Software for Orthogonal Distance Regression, NISTIR 4834, National Institute of Standards and Technology, Gaithersburg, MD, 1992.
- ⁷²M. L. Huber, *Comput. Chem. Eng.* **18**, 929 (1994).
- ⁷³M. Lundy and A. Mees, *Math. Program.* **34**, 111 (1986).
- ⁷⁴D. G. Friend and J. C. Rainwater, *Chem. Phys. Lett.* **107**, 590 (1984).
- ⁷⁵J. V. Sengers and J. M. H. Levelt Sengers, *Ann. Rev. Phys. Chem.* **37**, 189 (1986).
- ⁷⁶M. A. Anisimov, J. V. Sengers, and J. M. H. Levelt Sengers, “Near-critical behavior of aqueous systems,” in *Aqueous Systems at Elevated Temperatures and Pressures: Physical Chemistry in Water, Steam and Hydrothermal Solutions*, edited by D. A. Palmer, R. Fernández-Prini, and A. H. Harvey (Elsevier, Amsterdam, 2004), Chap. 2, pp. 29–71.
- ⁷⁷M. E. Fisher, *J. Math. Phys.* **5**, 944 (1964).
- ⁷⁸A. Kostrowicka Wyczalkowska, Kh. S. Abdulkadriova, M. A. Anisimov, and J. V. Sengers, *J. Chem. Phys.* **113**, 4985 (2000).
- ⁷⁹J. V. Sengers and J. G. Shanks, *J. Stat. Phys.* **137**, 857 (2009).
- ⁸⁰R. S. Basu, J. V. Sengers, and J. T. R. Watson, *Int. J. Thermophys.* **1**, 33 (1980).

- ⁸¹J. K. Bhattacharjee, R. A. Ferrell, R. S. Basu, and J. V. Sengers, *Phys. Rev. A* **24**, 1469 (1981).
- ⁸²J. V. Sengers and R. A. Perkins, "Fluids near critical points," in *Advances in Transport Properties of Fluids*, edited by M. J. Assael, A. R. H. Goodwin, V. Vesovic, and W. A. Wakeham (Royal Society of Chemistry, Cambridge, UK, 2014), Vol. 9, Chap. 10, pp. 337–361.
- ⁸³H. Hao, R. A. Ferrell, and J. K. Bhattacharjee, *Phys. Rev. E* **71**, 021201 (2005).
- ⁸⁴T. Ohta, *J. Phys. C: Solid State Phys.* **10**, 791 (1977).
- ⁸⁵H. C. Burstyn, J. V. Sengers, J. K. Bhattacharjee, and R. A. Ferrell, *Phys. Rev. A* **28**, 1567 (1983).
- ⁸⁶J. Luettmer-Strathmann, J. V. Sengers, and G. A. Olchowy, *J. Chem. Phys.* **103**, 7482 (1995).
- ⁸⁷G. A. Olchowy and J. V. Sengers, *Phys. Rev. Lett.* **61**, 15 (1988).
- ⁸⁸E. P. Sakonidou, H. R. van den Berg, C. A. ten Seldam, and J. V. Sengers, *J. Chem. Phys.* **105**, 10535 (1996).
- ⁸⁹M. R. Moldover, J. V. Sengers, R. W. Gammon, and R. J. Hocken, *Rev. Mod. Phys.* **51**, 79 (1979).
- ⁹⁰R. F. Berg, M. R. Moldover, and G. A. Zimmerli, *Phys. Rev. E* **60**, 4079 (1999).
- ⁹¹J. V. Sengers, R. A. Perkins, M. L. Huber, and D. G. Friend, *Int. J. Thermophys.* **30**, 374 (2009).
- ⁹²S. L. Rivkin, A. Y. Levin, and L. B. Izrailevskii, *Teplofiz. Svoistva Veshchestv Mater.* **10**, 232 (1976).
- ⁹³H. R. van den Berg, C. A. ten Seldam, and P. S. van der Gulik, *Physica A* **167**, 457 (1990).
- ⁹⁴H. R. van den Berg, C. A. ten Seldam, and P. S. van der Gulik, *J. Fluid Mech.* **246**, 1 (1993).
- ⁹⁵H. R. van den Berg, C. A. ten Seldam, and P. S. van der Gulik, *Int. J. Thermophys.* **14**, 865 (1993).
- ⁹⁶M. R. Mustafaev, *High Temp.* **34**, 130 (1996).
- ⁹⁷S. L. Rivkin (personal communication to J.V. Sengers, All-Union Heat Engineering Institute, Moscow, 1984).
- ⁹⁸R. A. Perkins, J. V. Sengers, I. M. Abdulagatov, and M. L. Huber, *Int. J. Thermophys.* **34**, 191 (2013).
- ⁹⁹A. Dehaoui, B. Issenmann, and F. Caupin, *Proc. Natl. Acad. Sci. U. S. A.* **112**, 12020 (2015).